mathematics

MDPI

Article

A Mixed-Integer Programming Framework for Drone Routing and Scheduling with Flexible Multiple Visits in Highway Traffic Monitoring

Nasrin Mohabbati-Kalejahi [1], Sepideh Alavi [2] and Oguz Toragay [3,*]

[1] Department of Information Systems, Lam Family College of Business, San Francisco State University, San Francisco, CA 94132, USA; mohabbati@sfsu.edu
[2] School of Cyber and Decision Sciences, Jack H. Brown College of Business and Public Administration, California State University, San Bernardino, CA 92407, USA; sepideh.alavi@csusb.edu
[3] Great Valley School of Graduate Professional Studies, The Pennsylvania State University, Malvern, PA 19355, USA
* Correspondence: ojt5116@psu.edu

Abstract

Traffic crashes and congestion generate high social and economic costs, yet traditional traffic monitoring methods, such as police patrols, fixed cameras, and helicopters, are costly, labor-intensive, and limited in spatial coverage. This paper presents a novel Drone Routing and Scheduling with Flexible Multiple Visits (DRSFMV) framework, an optimization model for planning drone-based highway monitoring under realistic operational constraints, including battery limits, variable monitoring durations, recharging at a depot, and target-specific inter-visit time limits. A mixed-integer nonlinear programming (MINLP) model and a linearized version (MILP) are presented to solve the problem. Due to the NP-hard nature of the underlying problem structure, a heuristic solver, Hexaly, is also used. A case study using real traffic census data from three Southern California counties tests the models across various network sizes and configurations. The MILP solves small and medium instances efficiently, and Hexaly produces high-quality solutions for large-scale networks. Results show clear trade-offs between drone availability and time-slot flexibility, and demonstrate that stricter revisit constraints raise operational cost.

Keywords: drone routing and scheduling; Unmanned Aerial Vehicles (UAVs); traffic monitoring; mixed-integer nonlinear programming (MINLP)

MSC: 90B06

Academic Editor: Andrea Scozzari

Received: 19 June 2025
Revised: 24 July 2025
Accepted: 25 July 2025
Published: 28 July 2025

Citation: Mohabbati-Kalejahi, N.; Alavi, S.; Toragay, O. A Mixed-Integer Programming Framework for Drone Routing and Scheduling with Flexible Multiple Visits in Highway Traffic Monitoring. *Mathematics* **2025**, *13*, 2427. https://doi.org/10.3390/math13152427

1. Introduction

Traffic accidents and emergencies pose significant challenges for public safety officials and transportation authorities. According to the National Highway Traffic Safety Administration [1], an estimated 5.9 million police-reported motor vehicle traffic crashes occurred in 2022, resulting in approximately 2.38 million injuries and 43,000 fatalities in the U.S. Despite improvements in road infrastructure and vehicle safety technology, accidents continue to occur with alarming frequency, causing injury, loss of life, and significant disruptions to traffic flow [2]. Traditional methods of traffic monitoring and management, such as manual observation by police patrols or helicopters or using traffic cameras, are costly and limited in their coverage. For instance, the Los Angeles Police Department's Air Support Division allocates $46.6 million annually to its operations, amounting to approximately

$127,805 per day or $2916 per flight hour to maintain its helicopters operational nearly non-stop, even for events considered non-high-priority [3]. California cities spent more than $15.1 billion on policing in the 2022–23 fiscal year, while counties spent $7.8 billion and the state spent $3 billion on the California Highway Patrol (CHP) [4]. Moreover, the increasing demand for police services, particularly in urban areas, further increases the challenge. Law enforcement agencies face limited resources, including funding, personnel, and equipment, making it difficult to allocate sufficient resources to traffic monitoring and enforcement. According to the Public Policy Institute of California [4], the number of patrol officers per 100,000 in the state is near its lowest point since 1991. Police departments are often stretched thin, struggling to assign enough officers to traffic duties. Traffic monitoring and enforcement are time-consuming and labor-intensive, requiring officers to spend long hours on the road. Furthermore, it is reported that the daily proactive efforts of police patrols on highways do not necessarily impact the frequency of traffic accidents in pre-identified incident hotspots [5]. Consequently, when crime rates are high or there are specific threats to public safety, police departments may prioritize these issues over traffic monitoring, further reducing the resources available for traffic management.

Logistical challenges pose significant obstacles to effective traffic monitoring and emergency response. Coordinating patrols across multiple jurisdictions and responding to emergencies or accidents in a timely manner are complex tasks, further complicated by factors such as traffic congestion, road construction, and inclement weather. The U.S. Department of Transportation Federal Highway Administration [6] emphasizes that ineffective access to accident scenes can substantially delay critical response times. The continuous monitoring of incident locations is essential for sharing real-time data with responders and law enforcement. Moreover, responders face considerable safety hazards while attending to road incidents, including working near moving traffic and dealing with hazardous materials, which can have severe consequences, such as the leakage of poisonous gases or explosion and fire risks [7]. A swift investigation of the incident locations is crucial for assessing the state of the road and identifying necessary actions. However, emergency response teams often struggle to quickly and accurately evaluate accident scenes, leading to delays in response times and potentially escalating the impact of accidents.

Given these challenges, some law enforcement agencies and transportation authorities are exploring alternative methods of traffic monitoring and enforcement, such as using drones, also known as Unmanned Aerial Vehicles (UAVs), to supplement traditional police patrols and provide additional data for transportation planning and management. Drones offer several significant advantages for traffic monitoring. They can cover a wider area than traditional methods [8] and can be easily repositioned to monitor emerging traffic hotspots [9]. Their deployment reduces the risk of accidents and injuries to human traffic monitors, and they are capable of providing real-time, high-quality visual data on accident scenes and traffic flow [10]. In addition to identifying areas of congestion as it develops [11], drones are also a cost-effective alternative to conventional monitoring systems and are environmentally friendly due to their lack of harmful emissions [12].

Although drones offer a transformative solution, their effective deployment is far from straightforward. The routing and scheduling of drones for traffic monitoring is a highly complex problem, influenced by factors such as limited battery life, traffic conditions, coverage requirements, and other constraints. These challenges necessitate practical mathematical models and optimization techniques that can handle the spatiotemporal complexity of the task while delivering actionable, real-time insights to decision-makers. This paper presents a novel approach to address these challenges by developing a new mathematical model for the routing and scheduling of drones in traffic monitoring.

Substituting drones for ground patrols ensures the timely inspection of high-risk locations, enables more agile responses to highway incidents, and reduces environmental impact. This also alleviates police staffing shortages and lowers overall patrol costs for routine monitoring strategies. Ultimately, the proposed solution demonstrates the critical role of emerging technologies in shaping the future of mobility and public safety.

The structure of the paper is organized as follows. Section 2 provides a review of the literature on drone applications in traffic monitoring. Section 3 introduces the proposed nonlinear mathematical model and its linearized equivalent. Section 4 presents the computational experiments and results, demonstrating the effectiveness of the proposed models. Finally, Section 5 summarizes the key findings, draws conclusions, and outlines directions for future research.

2. Drone-Based Traffic Monitoring: Insights from the Literature

The usage of drones has experienced rapid growth due to several compelling factors. Their exceptional mobility enables access to hard-to-reach areas and navigation through diverse terrains, which makes them invaluable across various sectors, including agriculture [13,14], disaster management [15–17], and logistics [18–21]. The remarkable flexibility of drones in terms of applications is noteworthy; they can be equipped with an array of sensors and cameras, allowing them to perform a wide spectrum of tasks ranging from aerial photography and videography to scientific research, traffic monitoring, and environmental assessment. Furthermore, drones offer significant environmental benefits by reducing the reliance on large, fuel-consuming vehicles and facilitating the more efficient monitoring and management of natural resources. This combination of mobility, versatility, and environmental advantages has driven their widespread adoption across multiple industries. The unique capabilities of drones position them as transformative technology in fields such as traffic monitoring and management, where traditional methods face limitations in terms of cost, coverage, and effectiveness.

The application of drones in traffic monitoring has gained significant attention due to their ability to address transportation challenges and respond to traffic bottlenecks in real time, surpassing traditional surveillance methods [22]. The literature on traffic monitoring and emergency response using drones can be broadly categorized into two main streams: (1) studies focused on capturing and analyzing data, images, and videos for decision-making, and (2) research developing mathematical models for routing, scheduling, and location decisions of drones on road networks.

2.1. Monitoring Applications of Drones in Traffic Systems

In the first category, several studies have explored various aspects of data collection and analysis. Khan et al. [23] examined hardware and software requirements for safe and efficient road traffic monitoring using UAVs. Elloumi et al. [24] studied how using multiple UAVs for road traffic monitoring improves performance and coverage rates compared to fixed drone trajectories. Barmpounakis and Geroliminis [25] created a large-scale urban dataset in Athens and conducted the pNEUMA experiment, which recorded traffic streams in a multi-modal congested environment using drones. Outay et al. [26] discussed advanced computer vision algorithms for extracting features from UAV footage and improving traffic flow analysis. Khan et al. [27] proposed a new model for monitoring speed limits and traffic violations using UAVs and 5G technology, demonstrating its effectiveness in reducing accidents by addressing traffic violations. Ahmed et al. [28] developed a process to overcome the limitations of vision algorithms in traffic monitoring, especially in areas with a high number of motorcycles and weak lane discipline, proposing a method to better capture heterogeneous vehicle stream data. Beg et al. [29] proposed a more

intelligent, autonomous UAV-enabled solution using simulation, considering scenarios such as traffic light violations, accident detection, mobile speeding traps, automated notifications, congestion detection, traffic rerouting, flagged stolen vehicles, pending arrest warrants, and vehicle tracking using UAVs and autonomous emergency response handling systems. Kumar et al. [30] introduced an innovative, lightweight, security-enabled distributed software-defined drone network (SDDN) for traffic monitoring where the security of drone/UAV communication and data exchange is ensured through a lightweight key generation and encryption/decryption algorithm. Kainz et al. [31] studied road traffic analysis through the detection of vehicles from the user-defined region of interest (ROI), employing the YOLOv4 model for vehicle detection after motion detection. Butilua et al. [32] provided a comprehensive review of UAV applications in civil engineering, including traffic monitoring and vehicle detection. Bisio et al. [33] conducted a systematic review of drone-based traffic monitoring systems from a deep learning perspective, focusing on vehicle detection, tracking, and counting.

2.2. Routing and Scheduling Models for Drone-Based Surveillance

The second category of research focuses on developing mathematical models for drone routing and scheduling. Conventional traffic monitoring methods rely on sensors installed in the road network, such as video cameras and inductive loop detectors, to monitor traffic movement. These sensors are typically fixed in specific locations, limiting their ability to gather comprehensive information about traffic patterns, such as an overall view of traffic flows, vehicle routes, and road network design [34]. These limitations highlight the importance of using drones as mobile solutions, which can provide more effective coverage. Consequently, the routing and scheduling of mobile UAVs to cover various areas and monitor locations have become key research areas.

Several papers investigate the cooperative use of ground vehicles (GVs) and drones in traffic monitoring. In these studies, the GV acts as a mobile base for launching, recovering, and charging the drones, which then inspect sections of the road network. These papers include developing a real-time data-driven approach through the first deterministic arc-inventory routing problem and deriving a stochastic dynamic policy for city monitoring during major events (Chow [35]), proposing a two-echelon cooperative routing problem for one ground vehicle and one UAV in urban road network monitoring (Luo et al. [36]), solving a vehicle-assisted multi-drone routing and scheduling problem (Hu et al. [37]), developing a patrol model where specific points and arcs can be accessed in the urban road network (Luo et al. [38]), and investigating a GV–drone arc routing problem (GVD-ARP) which considers a GV and multiple drones (Xu et al. [39]). While the use of ground vehicles (GVs) as mobile platforms for drone recovery and recharging offers certain advantages, their effectiveness diminishes in large part due to congested highway traffic networks. GVs often struggle to navigate swiftly through dense traffic, potentially amplifying congestion issues. Furthermore, existing studies frequently make simplifying assumptions, such as negligible recharging and monitoring times, and typically restrict drones to visiting a single node after each vehicle takeoff.

Researchers have developed various models to enhance the effectiveness of drone usage in traffic monitoring. Zhang et al. [40] proposed a model for a dynamically configured sensor network that accounts for time-varying traffic flow propagation, expanding both spatially and temporally. They developed a UAV routing and scheduling model integrated with existing fixed traffic monitoring sites, aiming to minimize the total cost in terms of detection delay for spatially and temporally distributed incidents. Ghazzai et al. [41] developed a generic scheduling framework for UAVs to cover multiple events with minimal energy consumption. Their approach optimizes the schedule by determining

which UAVs will sequentially cover each event, the time each UAV spends at an event, waiting times, battery charging at docking stations, and the start times of their trips. Building on this, Ghazzai et al. [42] proposed a model to optimize the location of charging stations, considering the flying time to incident locations and the risk of battery failure during operations. They also developed a proactive scheduling framework to minimize total energy consumption while achieving specific coverage efficiency by visiting each target only once. Christodoulou and Kolios [43] tackled a set covering problem in road traffic monitoring. Their model does not account for temporal factors, so nodes do not have specific visit time requirements. The problem focuses solely on determining the minimum number of tours needed to cover the monitoring locations within a finite tour cost. Kumar et al. [44] explored collision-free drone movement strategies for road traffic monitoring using Software-Defined Networking (SDN). The SDN-controlled drone network reduces overhead and improves drone-device management. Their simulations were conducted using OpenFlow version 1.3.x and protocol version 0x04. Rigas et al. [45] proposed a drone scheduling framework for monitoring missions in transportation networks, where monitoring locations must be visited at specific, predefined time points. Their model represented the monitored area as a graph with nodes denoting demand or supply locations, and incorporates energy constraints by requiring battery replacements at designated supply nodes after limited flight durations. The focus is on maximizing the number of time-specific monitoring demands satisfied within a centralized, discrete-time scheduling framework.

The problem of locating and routing UAVs at the tactical level was studied by Yakıcı et al. [46] to maximize the total score obtained from visited demand points by flight routes of UAVs. The problem considers assigning UAVs to base stations and finding optimal routes to serve the demand points. Terzi et al. [47] proposed a framework for intelligent multi-drone tasking in emergency response missions with the goal of minimizing the total fly time cost under the limited fly time duration of each agent and the demands set by the set of tasks. Each drone has to stay over each location for a specific period of time and should take off and land at the depot. They approach the problem using a variation of the VRP and consider routes on a graph of nodes and edges; task requirements are modeled as costs on the edges and as demands on nodes visited. These studies primarily focus on single visits to locations within the planning horizon, neglecting the crucial aspect of repeated visits to points of interest, which is a key requirement in effective road traffic monitoring and emergency situation detection.

In the context of traffic monitoring using drones, some studies focus on route optimization, modeling the problem as an arc routing problem or traveling salesman problem (Elloumi et al. [24], Oh et al. [48], Campbell et al. [49], Luo et al. [38], Xu et al. [39]). In these studies, roads requiring traffic monitoring are represented as nodes or arcs in a network. The objective is for one or more UAVs to traverse these nodes or arcs, aiming to minimize flight time or battery consumption. To optimize UAV monitoring routes during rush hours, Wang et al. [50] developed a route planning method that accounts for spatiotemporal variations in monitoring demand and introduced a team orienteering arc routing problem with time-varying profits. Li et al. [22] proposed an optimization model for traffic monitoring aimed at minimizing the total expected operational costs. Their approach involves a capacitated arc routing problem and an inventory routing problem, dynamically assigning UAVs to monitor uncertain demand arcs across multiple periods. Cheng et al. [51] presented a task assignment model for road patrols using multiple UAVs with various bases and rechargeable endurance. This model aims to minimize the time required to complete all tasks, considering the mission as complete only when every mission point has been patrolled, and the deadline is defined by the time that it takes for the last drone to return to its nearest base. Additionally, each drone is restricted from patrolling the same target point

repeatedly. Huang et al. [52] proposed a decentralized, real-time approach for navigating a team of UAVs for road traffic monitoring. In their scenario, the UAVs exchange position and measurement information only with their neighboring UAVs.

Studies on highway patrol using drones are limited. Niu et al. [53] formulated a multi-objective optimization model for routing multiple UAVs to collect traffic information, aiming to minimize flight time and uncollected data, but lacked an algorithm for actual highway instances. Jo et al. [54] designed an efficient drone patrol network system using the OPNET simulator. Li et al. [55] proposed using UAVs to gather information in blind areas where smart vehicles cannot derive real-time data, focusing on task assignments without considering drone routing. Kim et al. [56] presented an integer programming model to optimize drone schedules for the Gyeongbu Expressway in Korea. Choi et al. [57] presented two integer programming formulations, basic and path-based, to create an operational schedule for multiple highway patrol drones to meet varying patrol demands across different highway sections and times. The objective of their study is to determine the operation schedule of patrol drones that can meet the patrol demand in sections that change over time during the planning horizon. These studies lack considerations such as operational flexibility, recharging, and continuous traffic monitoring.

This study proposes a novel optimization model called Drone Routing and Scheduling with Flexible Multiple Visits (DRSFMV), which captures the operational complexities of real-world highway traffic monitoring. The model incorporates location-specific maximum inter-visit time constraints to support continuous and adaptive monitoring. Unlike prior models that assume single visits or overlook drone-specific limitations, our formulation integrates critical operational features such as variable drone speeds based on task type, heterogeneous monitoring durations, battery constraints with explicit recharging operations, and the option for drones to remain idle when strategically beneficial. By doing so, the proposed model reflects practical deployment conditions and offers a flexible scheduling framework that enhances surveillance reliability.

Table 1 summarizes the reviewed literature and highlights the contributions and novelty of the proposed problem.

Table 1. Comparison of previous studies with the proposed DRSFMV model.

Study	Objective Function	Repeated Visits	Battery Recharge	Max Inter-Visit Time	Heterogeneous Monitoring Durations
Fan et al. (2022) [34]	Minimize routing cost via DRL	✗	✓	✗	✗
Chow (2016) [35]	Minimize stochastic routing cost	✗	✗	✗	✗
Luo et al. (2017) [36]	Minimize 2-echelon routing cost	✗	✓ (GV)	✗	✗
Hu et al. (2018) [37]	Joint routing and scheduling	✗	✓	✗	✗
Luo et al. (2019) [38]	Minimize patrol cost	✗	✗	✗	✗
Xu et al. (2023) [39]	GV-drone arc routing	✗	✗	✗	✗
Zhang et al. (2015) [40]	Minimize detection delay	✗	✓	✗	✗
Ghazzai et al. (2018) [41]	Minimize energy usage	✗	✓	✗	✗
Ghazzai et al. (2019) [42]	Proactive energy scheduling	✗	✓	✗	✗

Table 1. *Cont.*

Study	Objective Function	Repeated Visits	Battery Recharge	Max Inter-Visit Time	Heterogeneous Monitoring Durations
Christodoulou & Kolios (2020) [43]	Minimize number of tours	✗	✗	✗	✗
Kumar et al. (2021) [44]	Secure communication (SDDN)	✗	✗	✗	✗
Rigas et al. (2021) [45]	Max. time-specific coverage	✓ (fixed)	✓	✗	✗
Yakıcı (2016) [46]	Maximize visit score	✗	✗	✗	✗
Terzi et al. (2019) [47]	Minimize total flight time	✗	✗	✗	✓
Oh et al. (2014) [48]	Minimize route cost	✗	✗	✗	✗
Campbell et al. (2021) [49]	Minimize postman cost	✗	✗	✗	✗
Wang et al. (2022) [50]	Maximize time-based coverage	✗	✗	✗	✗
Cheng et al. (2019) [51]	Minimize patrol completion time	✗	✓	✗	✗
Huang et al. (2021) [52]	Decentralized coverage	✗	✗	✗	✗
Niu et al. (2015) [53]	Minimize UAV flight	✗	✗	✗	✗
Jo (2017) [54]	Patrol network simulation	✗	✗	✗	✗
Li et al. (2020) [55]	UAV blind-spot coverage	✗	✗	✗	✗
Kim et al. (2022) [56]	Highway drone scheduling	✗	✓	✗	✗
Choi et al. (2024) [57]	Time-varying patrol coverage	✓ (not flexible)	✓	✗	✗
This study (DRSFMV)	Minimize maximum lateness and earliness of visits	✓	✓	✓	✓

3. Problem Formulation and Model Development

The Drone Routing and Scheduling with Flexible Multiple Visits (DRSFMV) proposed in this paper is designed based on practical requirements that have not been fully addressed in previous research, such as repeated visits with inter-visit time constraints, battery limitations, and recharging operations. To facilitate the understanding of the problem, first, the key features of the problem are presented, followed by the introduction of a novel mixed-integer nonlinear mathematical model. A linear equivalent formulation is also proposed to enable the problem to be efficiently solved using commercial solvers.

3.1. Problem Description and Key Assumptions

The proposed model assumes a fleet of $\mathcal{M}$ identical drones for traffic monitoring, tasked with visiting Q targets multiple times over a 24 h period. These targets, representing arcs on a road network, require repeated visits due to their status as traffic bottlenecks or areas with high accident probabilities. Visiting requirements are different for each target in terms of both frequency and specific timing during the day.

To model multiple visits to each location, each visit is considered as a different node in the network with the exact specifications of that target $q \in Q$. Let F_q^v denote the set of all visits v for each target $q \in Q$. The time length of the visit is unique for each target $q \in Q$ and calculated based on the length of the arc in the road network, but identical for

all visits in F_q^v. The time required for a drone to fly from target j to target k is represented by s_{jk}. Note that arcs have visiting directions, so flight times are calculated based on the distance between the end point of the arc j to the start point of the arc k, which makes the distance matrix asymmetric. Each drone spends a specific duration monitoring the visited target, which may involve surveying an arc of the road network. Consequently, a monitoring time p_{jri} is considered for each visit of each drone. For the model to be more realistic, various drone speeds are considered for different tasks. More specifically, it is assumed that, while monitoring targets to record high-quality videography, the drones fly at a lower speed than the times that they fly between different targets or fly to/from the depot. A maximum inter-visit time, I_q, is introduced for each target $q \in Q$, which shows the maximum allowable time interval between consecutive visits to target q, measured from the completion of one visit to the start of the next visit. This parameter is crucial to maintain consistent surveillance and ensure the timely monitoring of critical locations within the network. This differs from the regular time window assumptions in the literature, where time window constraints specify the start and end times of a visit as an interval. By incorporating these time-related constraints, our model achieves a balance between comprehensive coverage and operational efficiency, allowing adaptive scheduling that responds to the dynamic nature of traffic patterns and potential emergency situations.

An asymmetrical distance matrix is created, where each entry shows the travel distance from the end point of an origin route to the start point of a destination route. This reflects the actual flight path that a drone follows after completing one monitoring task and moving to the next. Additionally, it is assumed that a drone cannot visit the same location consecutively, as this would mean staying in the same place in a row. To prevent this, a large penalty (100,000) is set on the main diagonal of the distance matrix. This discourages assigning consecutive visits to the same node by greatly increasing the associated travel time.

A fixed location is considered as the depot in the model from which drones initiate their routes and return for recharging as needed. Additionally, a set of dummy nodes is introduced where drones remain idle. Unlike road segment targets, idle nodes are conceptual placeholders that do not consume battery charge, can be visited at any point in the schedule, and are not restricted by a maximum number of visits. Furthermore, the duration of a drone's stay at an idle node is considered a continuous decision variable, g_{jri} ($\forall j \in \{idle\}$). The purpose of defining these nodes is related to the solution decoding process. A feasible solution to the problem is represented by defining R available slots for each drone's visit sequence. The model requires that each slot be assigned to exactly one visit, while satisfying all operational constraints such as inter-visit time limits and avoiding consecutive visits to the same target. This approach offers flexibility within a structured routing framework, ensuring that the model can incorporate all scheduling constraints while remaining feasible.

Our defined problem has some overlaps with the many-visits multiple traveling salesman problem, which is a new concept proposed in 2023 in the literature [58]. In this problem, each city has a fixed number of visits requested, and there are m salesmen who need to visit different cities multiple times. However, our proposed problem is more complex in the sense that there is a maximum inter-visit time between multiple visits to each target. In addition, drones require charging, which significantly changes the dynamics of the routing problem.

Table 2 shows the sets, parameters, and decision variables used in the proposed mathematical models.

Table 2. Notation of the proposed mathematical model.

Sets and Parameters	
F_q^v	Set of visits v for each target q
M	Number of identical drones
Q	Number of targets
N	Number of visits to all targets $= \sum_v \sum_q F_q^v$
R	Number of defined slots on each drone
i	Index set of drones, where $i \in M = \{1, \ldots, M\}$
j, k	Index set of visits, where $j, k \in N = \{1, \ldots, N\}$
r	Index set of slots on each drone, where $r \in R = \{1, \ldots, R\}$
t_{kj}	Travel time between visits k and j
p_{jri}	Monitoring time for target j on slot r of drone i; $j \notin idle$
e_j	The earliest possible start time for visit j
d_j	The due date of visit j
I_q	Maximum inter-visit time between consequent visits to target q
fc	Total flight time of a fully charged drone
UB	Upper bound for the dummy variables
LB	Lower bound for the dummy variables
Decision Variables	
x_{jri}	1 if visit j is assigned to the slot r on drone i; 0 otherwise
c_{ri}	The completion time of monitoring a target on slot r of drone i
s_{ri}	The start time of monitoring a target on slot r of drone i
h_{ri}	Remaining charge in drone i after completing a visit assigned to slot r
$g_{idle,r,i}$	Time spent on node $idle$ on slot r of drone i
L_{max}	The maximum lateness
E_{max}	The maximum earliness
u_{jri}	Dummy variable to linearize $g_{jri} \times x_{jri}$
v_{ri}	Dummy variable to linearize $(h_{(r-1)i} + c_{(r-1)i}) \times x_{jri}$
w_{ri}	Dummy variable to linearize $c_{ri} \times x_{jri} \quad \forall j \in N - \{1, idle\}$
y_{jkri}	Dummy variable to linearize $x_{jri} \times x_{k(r-1)i}$
z_{ri}	Dummy variable to linearize $s_{ri} \times x_{jri} \quad \forall j \in \{idles\}$
a_{jri}	Dummy variable to linearize $s_{ri} \times x_{jri}, \quad \forall j \in F_q^v$
b_{jri}	Dummy variable to linearize $c_{ri} \times x_{jri}, \quad \forall j \in F_q^v$

3.2. Mathematical Formulation: Nonlinear Model

The proposed mixed-integer nonlinear model is presented below. Later, the linear equivalent of the model is presented to compare the run time and convergence of the two modeling approaches.

$$\min \quad L_{max} + E_{max}$$

s.t.

$$L_{max} \geq c_{ri} - \sum_{j \in N} (d_j \times x_{jri}), \quad \forall r \in R, i \in M \tag{1}$$

$$E_{max} \geq \sum_{j \in N} (e_j \times x_{jri}) - s_{ri}, \quad \forall r \in R, i \in M \tag{2}$$

$$\sum_{r \in R} \sum_{i \in M} x_{jri} = 1, \quad \forall j \in N - \{1, idle\} \tag{3}$$

$$\sum_{j \in N} x_{jri} = 1, \quad \forall i \in N, r \in R \tag{4}$$

$$c_{1i} = \sum_{j \in N} (t_{1j} \times x_{j1i}) + \sum_{j \in N - idle} (p_{j1i} \times x_{j1i}) + \sum_{j \in idle} (g_{j1i} \times x_{j1i}), \quad \forall i \in M \tag{5}$$

$$c_{ri} = c_{(r-1)i} + \sum_{j \in N} \sum_{k \in N} (t_{kj} \times x_{jri} \times x_{k(r-1)i}) + \sum_{j \in N - idle} (p_{jri} \times x_{jri}) + \sum_{j \in idle} (g_{jri} \times x_{jri}), \quad \forall r \in R - \{1\}, i \in M \tag{6}$$

$$s_{1i} = 0, \quad \forall i \in M \tag{7}$$

$$s_{ri} = c_{ri} - \sum_{j \in N - idle} (p_{jri} \times x_{jri}) + \sum_{j \in idle} (g_{jri} \times x_{jri}), \quad \forall r \in R - \{1\}, i \in M \tag{8}$$

$$h_{1i} = fc - \sum_{j \in N} (t_{1j} \times x_{j1i}) - \sum_{j \in N - idle} (p_{j1i} \times x_{j1i}), \quad \forall i \in M \tag{9}$$

$$h_{ri} = (fc \times x_{1ri}) + (h_{(r-1)i} - c_{ri} + c_{(r-1)i}) \times \sum_{j \in N - \{1, idle\}} x_{jri} + (h_{(r-1)i} - s_{ri} + c_{(r-1)i}) \times \sum_{j \in \{idle\}} x_{jri}, \quad \forall r \in R - \{1\}, i \in M \tag{10}$$

$$\sum_{r \in R} \sum_{i \in M} (s_{ri} \times x_{(j+1)ri}) - \sum_{r \in R} \sum_{i \in M} (c_{ri} \times x_{jri}) \leq I_q, \quad \forall j \in F_q^v \tag{11}$$

$$\sum_{r \in R} \sum_{i \in M} (s_{ri} \times x_{(j+1)ri}) - \sum_{r \in R} \sum_{i \in M} (c_{ri} \times x_{jri}) \geq 0, \quad \forall j \in F_q^v \tag{12}$$

$$x_{jri} \in \{0, 1\}; c_{ri}, s_{ri}, h_{ri}, g_{idle,r,i}, L_{max}, E_{max} \geq 0, \quad \forall j \in N, i \in M, r \in R. \tag{13}$$

The objective function minimizes the maximum lateness and earliness of drone visits to all targets, based on pre-defined due dates and earliest possible start times. Constraint (1) calculates the maximum lateness by comparing each visit's completion time to its due date, while Constraint (2) determines the maximum earliness using the earliest possible times and visit start times. Constraint (3) ensures that each visit occurs only once, with exceptions for depot visits for charging or idle nodes. Constraint (4) assigns each visit to a single drone slot, preventing simultaneous multiple visits by a single drone. Constraints (5) and (6) compute visit completion times, incorporating travel time between targets (or between a target and the depot) and monitoring duration. Constraints (7) and (8) calculate the start time of each visit. Constraints (9) and (10) manage drones' battery levels, triggering depot returns for recharging when necessary. Constraints (11) and (12) ensure that the time difference between two consecutive visits to a target does not exceed the allowed maximum inter-visit time. Constraint (12) also guarantees that a visit to any target should

start after the previous visit to the same target has been completed. Constraint (13) shows the defined variables.

3.3. Linearization of the Model

In order to solve the model efficiently using commercial solvers, we attempt to linearize it. Constraints (5), (6), (8), (10), (11), and (12) are nonlinear. Their linear equivalents, along with the corresponding linearization process, are presented below.

Constraints (5) and (8) only have one nonlinear term, which is a multiplication of two nonnegative variables $g_{jri} \times x_{jri}$, and, therefore, need linearization. To linearize this term, a dummy variable $u_{jri} = g_{jri} \times x_{jri}$ is defined. The following constraints should replace the current versions of Constraints (5) and (8):

$$c_{1i} = \sum_{j \in N} (t_{1j} \times x_{j1i}) + \sum_{j \in N-idle} (p_{j1i} \times x_{j1i}) + \sum_{j \in idle} u_{j1i}, \quad \forall i \in M \tag{5a}$$

$$s_{ri} = c_{ri} - \sum_{j \in N-idle} (p_{jri} \times x_{jri}) + \sum_{j \in idle} u_{jri}, \quad \forall r \in R - \{1\}, i \in M \tag{8a}$$

The following equations demonstrate the implementation of the dummy variable u and should be added to the mathematical model:

$$u_{jri} \geq g_{jri} - UB(1 - x_{jri}), \quad \forall j \in idle, i \in M, r \in R \tag{14}$$

$$u_{jri} \leq g_{jri} + LB(1 - x_{jri}), \quad \forall j \in idle, i \in M, r \in R \tag{15}$$

$$u_{jri} \leq UB(x_{jri}), \quad \forall j \in idle, i \in M, r \in R \tag{16}$$

$$u_{jri} \geq LB(x_{jri}), \quad \forall j \in idle, i \in M, r \in R \tag{17}$$

Constraint (6) has two nonlinear terms: $g_{jri} \times x_{jri}$, which will be replaced by u_{jri}, and $x_{jri} \times x_{k(r-1)i}$, which will be replaced by a new dummy variable, y_{jkri}.

$$c_{ri} = c_{(r-1)i} + \sum_{j \in N} \sum_{k \in N} (t_{kj} \times y_{jkri}) + \sum_{j \in N-idle} (p_{jri} \times x_{jri}) + \sum_{j \in idle} u_{jri}, \quad \forall i \in M, r \in R - \{1\} \tag{6a}$$

The following equations should be added to the model as a way of defining the new dummy variable y and how it relates to the main decision variable x:

$$x_{jri} + x_{j(r-1)i} - 1 \leq y_{jkri}, \quad \forall r \in R, i \in M, j, k \in N, j \neq k \tag{18}$$

$$\frac{1}{2}(x_{jri} + x_{j(r-1)i}) \geq y_{jkri}, \quad \forall r \in R, i \in M, j, k \in N, j \neq k \tag{19}$$

Constraint (10) has three nonlinear terms: (a) $(h_{(r-1)i} + c_{(r-1)i}) \times x_{jri}$, (b) $c_{ri} \times x_{jri}$, and (c) $s_{ri} \times x_{jri} \forall j \in \{idles\}$, which are replaced with three dummy variables v_{ri}, w_{ri}, z_{ri}, accordingly. Constraint (10) should be replaced by the following constraint:

$$h_{ri} = (fc \times x_{1ri}) + v_{r1} - w_{ri} - z_{r1}, \quad \forall r \in R - \{1\}, i \in M \tag{10a}$$

The following constraints should be added to the model for definitions of the new dummy variables:

$$v_{ri} \leq (h_{(r-1)i} + c_{(r-1)i}) + (LB \times x_{1ri}), \quad \forall r \in R - \{1\}, i \in M \tag{20}$$

$$v_{ri} \geq (h_{(r-1)i} + c_{(r-1)i}) - (UB \times x_{1ri}), \quad \forall r \in R - \{1\}, i \in M \tag{21}$$

$$v_{ri} \leq UB \times (1 - x_{1ri}), \quad \forall r \in R - \{1\}, i \in M \tag{22}$$

$$v_{ri} \geq LB \times (1 - x_{1ri}), \quad \forall r \in R - \{1\}, i \in M \tag{23}$$

$$w_{ri} \leq c_{ri} + LB \times (1 - \sum_{j \in N - \{1, idle\}} x_{jri}), \quad \forall r \in R - \{1\}, i \in M \tag{24}$$

$$w_{ri} \geq c_{ri} - UB \times (1 - \sum_{j \in N - \{1, idle\}} x_{jri}), \quad \forall r \in R - \{1\}, i \in M \tag{25}$$

$$w_{ri} \leq UB \times \sum_{j \in N - \{1, idle\}} x_{jri}, \quad \forall r \in R - \{1\}, i \in M \tag{26}$$

$$w_{ri} \geq LB \times \sum_{j \in N - \{1, idle\}} x_{jri}, \quad \forall r \in R - \{1\}, i \in M \tag{27}$$

$$z_{ri} \leq s_{ri} + LB \times (1 - \sum_{j \in idle} x_{jri}), \quad \forall r \in R - \{1\}, i \in M \tag{28}$$

$$z_{ri} \geq s_{ri} - UB \times (1 - \sum_{j \in idle} x_{jri}), \quad \forall r \in R - \{1\}, i \in M \tag{29}$$

$$z_{ri} \leq UB \times \sum_{j \in idle} x_{jri}, \quad \forall r \in R - \{1\}, i \in M \tag{30}$$

$$z_{ri} \geq LB \times \sum_{j \in idle} x_{jri}, \quad \forall r \in R - \{1\}, i \in M \tag{31}$$

To linearize Constraints (11) and (12), two dummy variables $a_{jri} = s_{ri} \times x_{jri}, \forall j \in N - \{1, idle\}$ and $b_{jri} = c_{ri} \times x_{jri}, \forall j \in N - \{1, idle\}$ are defined. Then, they should be replaced by the following two constraints:

$$\sum_{r \in R} \sum_{i \in M} a_{(j+1)ri} - \sum_{r \in R} \sum_{i \in M} b_{jri} \leq I_n \quad \forall j \in F_q^n \tag{11a}$$

$$\sum_{r \in R} \sum_{i \in M} a_{(j+1)ri} - \sum_{r \in R} \sum_{i \in M} b_{jri} \geq 0, \quad \forall j \in F_q^n \tag{12a}$$

To define the dummy variables a_{jri} and b_{jir}, the following constraints should be added to the model:

$$a_{jri} \geq s_{ri} - UB \times (1 - x_{jri}) \quad \forall j \in F_q^n, i \in M, r \in R \tag{32}$$

$$a_{jri} \leq s_{ri} + LB \times (1 - x_{jri}) \quad \forall j \in F_q^n, i \in M, r \in R \tag{33}$$

$$a_{jri} \leq UB \times (x_{jri}) \quad \forall j \in F_q^n, i \in M, r \in R \tag{34}$$

$$a_{jri} \geq LB \times (x_{jri}) \quad \forall j \in F_q^n, i \in M, r \in R \tag{35}$$

$$b_{jri} \geq c_{ri} - UB \times (1 - x_{jri}) \quad \forall j \in F_q^n, i \in M, r \in R \tag{36}$$

$$b_{jri} \leq c_{ri} + LB \times (1 - x_{jri}) \quad \forall j \in F_q^n, i \in M, r \in R \tag{37}$$

$$b_{jri} \leq UB \times (x_{jri}) \quad \forall j \in F_q^n, i \in M, r \in R \tag{38}$$

$$b_{jri} \geq LB \times (x_{jri}) \quad \forall j \in F_q^n, i \in M, r \in R. \tag{39}$$

The final constraint should be the definition of the new dummy variables:

$$y_{jkri} \in \{0,1\}; u_{jri}, v_{ri}, w_{ri}, z_{ri}, a_{jri}, b_{jri} \geq 0, \quad \forall j,k \in N, i \in M, r \in R. \tag{40}$$

Therefore, the linear mixed-integer mathematical model is presented below.

$$\min \quad L_{max} + E_{max}$$

s.t.

$$(1), (2), (3), (4), (5a), (6a), (7), (8a), (9), (10a), (11a), (12a), (13), (14) - (40).$$

4. Computational Experiments and Performance Evaluation

The aim of the experimental study is to evaluate the performance of the proposed mixed-integer nonlinear programming (MINLP) formulation and its linear equivalent developed for the Drone Routing and Scheduling with Flexible Multiple Visits (DRSFMV) problem in the context of traffic monitoring. The experiments are conducted to assess three primary aspects: (i) the computational tractability of the model when applied to realistic urban-scale problem instances, (ii) the solution quality in terms of coverage efficiency and revisit compliance, and (iii) the model's comparative performance of different formulations using multiple solvers.

4.1. Case Study and Experimental Setup

The computational experiments are based on a case study of high-traffic routes in the Southern California region, using publicly available data from the California Government Traffic Census bottleneck database [59]. The study focuses on three major counties: San Bernardino (SB), Los Angeles (LA), and Riverside (RS). Specifically, the dataset includes four critical bottleneck segments in San Bernardino (SB1–SB4), four in Riverside (RS1–RS4),

and eight in Los Angeles (LA1–LA8). These road segments serve as the monitoring targets in the DRSFMV model. For each segment, we summed the vehicle-hours of delay over the 24 h period and allocated the necessary number of drone visits in proportion to the total delay. Segments with higher delay receive more visits. The dataset does not specify when each bottleneck occurs during the day. Therefore, we divided the 24-h period into eight equal 3-h segments and randomly assigned the visits for each target to those segments. The maximum inter-visit time is calculated by subtracting the end time of the first visit from the start time of the second visit and then adding a predefined threshold (30 min). This threshold prevents back-to-back visits to the same target.

Drones are considered to be operating at two distinct speeds, depending on their activity: 60 km/h when in transit between sites and 30 km/h during monitoring, reflecting the reduced speed needed for high-resolution visual capture.

A single centralized depot is used as the origin and return point for all drones. For the main depot, the police station closest to the geometric center of all targets, the Walnut/Diamond Bar Sheriff's Station was selected. We assumed that drones would launch, land, and recharge at this location. The geographic center of each county is calculated from the coordinates of its target group and designated as the idle node, allowing drones to wait there as long as needed without using battery power until their next assignment. In total, three idle nodes are considered, one in each county. These nodes, along with the depot and target locations, are illustrated in Figures 1 and 2, where boxed labels indicate the depot and idle points.

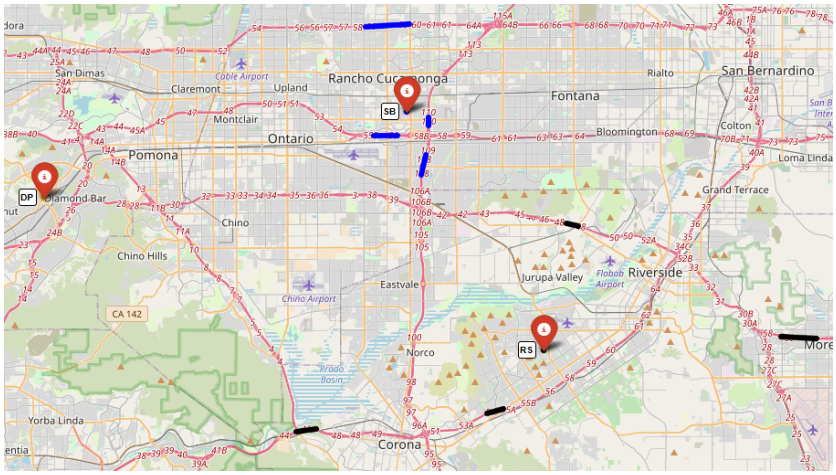

Figure 1. SB and RS monitoring targets map. Map data © OpenStreetMap contributors.

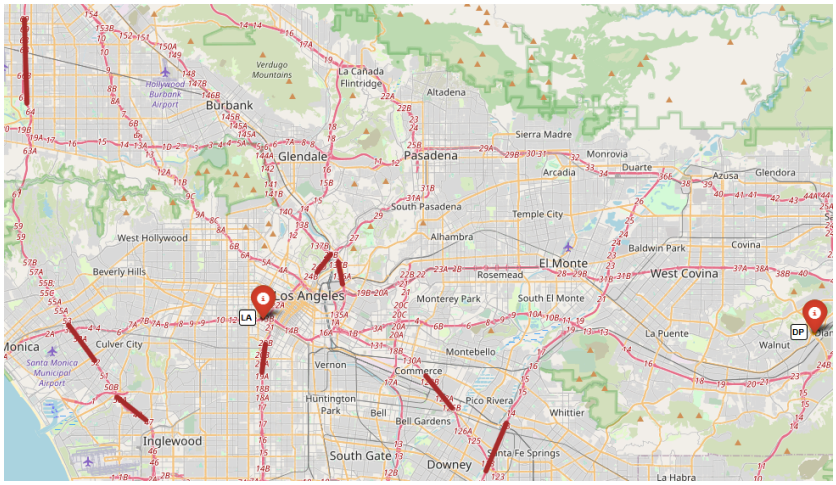

Figure 2. LA monitoring targets map. Map data © OpenStreetMap contributors.

The proposed DRSFMV formulation is implemented using the Pyomo optimization modeling framework [60], which supports the development of both linear and nonlinear variants of the model. To obtain exact solutions, the Gurobi solver [61] is employed, as it demonstrates strong performance across mixed-integer linear programming (MILP) and nonlinear programming (NLP) problems. Gurobi serves as the baseline solver in this study, offering benchmark solutions that inform the tractability and scalability of the DRSFMV model under varying configurations.

To extend the solution capability beyond small and moderately sized instances, we also incorporate the Hexaly optimization solver [62]. Hexaly is a next-generation hybrid solver designed to efficiently handle large-scale combinatorial optimization problems. It integrates local search heuristics, constraint programming, and machine learning—proven strategies to generate high-quality solutions within reasonable computation times [63].

The core scheduling sub-structure of the DRSFMV problem is at least as hard as the classical parallel machine scheduling problem with the objective of minimizing the maximum completion time ($P_m||C_{\max}$), which is known to be NP-hard [64]. Furthermore, when all job due dates are assumed to be at the beginning of the planning horizon, the $P_m||L_{\max}$ problem reduces to an equivalent formulation of $C_{\max}$ and thus remains NP-hard [65]. As a result, the solution time is expected to exhibit non-polynomial growth with respect to instance size, posing significant computational challenges for exact solution methods.

Given this complexity, traditional solvers such as *CPLEX*, *Gurobi*, and *SCIP*, which predominantly rely on branch-and-bound or branch-and-cut algorithms within linear programming frameworks, face difficulties when applied to highly combinatorial or nonlinear formulations. These methods are well-suited for structured linear problems but often fail to scale effectively under the nonlinear and interdependent constraints inherent in the DRSFMV problem [66]. To overcome these limitations, we leverage Hexaly's advanced hybrid search framework, which is particularly well-suited for non-convex and multi-level decision problems. By combining adaptive metaheuristics with parallel computation, Hexaly explores the solution space more efficiently and is capable of producing near-optimal or optimal solutions in significantly shorter run-times, even for complex, large-scale instances [67]. A comparative overview of Hexaly and conventional solvers is presented in Table 3, highlighting differences in algorithmic strategy, modeling flexibility, and empirical performance.

Table 3. Comparison of Hexaly and traditional solvers.

Feature	Hexaly	Traditional Solvers
Core Methodology	Hybrid local search with constraint propagation and learning-based heuristics	Branch-and-bound/cut with linear programming techniques
Problem Suitability	Excels in nonlinear, combinatorial, and large-scale problems	Best for linear and mixed-integer programming problems
Computation Speed	Faster for complex problems due to heuristic-driven exploration	Slower for large-scale, nonlinear problems
Solution Quality	Near-optimal or optimal, with trade-offs for speed	Optimal but may require significant time
Modeling Complexity	Intuitive, high-level language for complex constraints	Requires linearization or reformulation for nonlinear problems
Scalability	Highly scalable for millions of variables/constraints	Scalability limited by problem size and linearity

All experiments were conducted on a workstation equipped with an Intel(R) Core(TM) i9-12900K processor running at 3.20 GHz, with 64.0 GB of RAM, and operating on Windows 11 Pro. Python Optimization Modeling Object (Pyomo) version 6.7.0 is used for coding the mathematical models. Gurobi version 12.0.1 is used to solve MILP and MINLP models. For experiments using Hexaly, version 13.5 of the solver was executed. All experiments were run in a multi-threaded mode with 24 threads. No additional solver-specific tuning was applied unless otherwise noted.

4.2. Results and Comparative Analysis

To test the scalability and computational performance of the proposed model and solvers (i.e., LP, NLP, HX) under varying levels of complexity, we constructed three distinct problem sizes. The small-sized instance represents the simplest configuration, the medium-sized instance introduces moderate complexity, and the large-sized instance reflects the most comprehensive scenarios. These instances are designed to assess how the model handles increasing numbers of monitoring targets, required visits, and scheduling constraints. These instances were evaluated under different configurations of parameters, including the number of drones and slots, across 40 runs for each county and are presented in Tables 4–10.

Figures 3–9 present box plots that visualize the distribution of objective values obtained under different drone-slot configurations and model/solver types across small-, medium-, and large-sized problem instances. Each box plot corresponds to a specific configuration of the number of drones (M) and time slots (R). The central horizontal line within each box indicates the median objective value, while the lower and upper edges represent the first and third quartiles, respectively. The whiskers extend to the minimum and maximum values within 1.5 times the interquartile range, and individual points beyond this range are shown as outliers. These outliers reflect scheduling configurations where constraints such as tight inter-visit times or limited drone availability significantly impacted performance. In the context of the problem, lower objective values indicate a more effective alignment of drone scheduling with required revisit intervals and monitoring deadlines.

Tables 4 and 5 and Figures 3 and 4 present the results obtained from the small-sized problem instances in San Bernardino and Riverside.

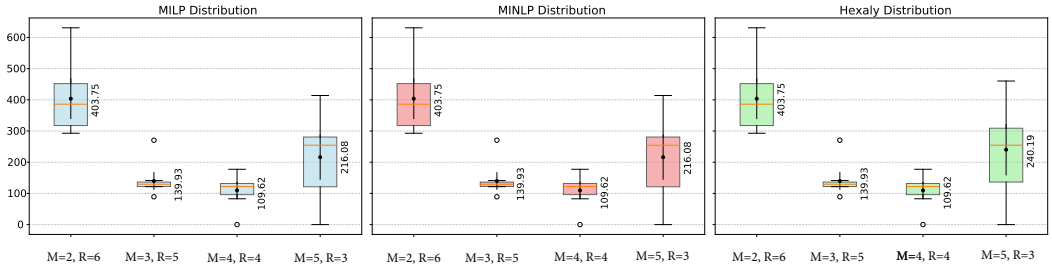

Figure 3. Distribution of objective values across drone-slot configurations (small-sized instances in San Bernardino).

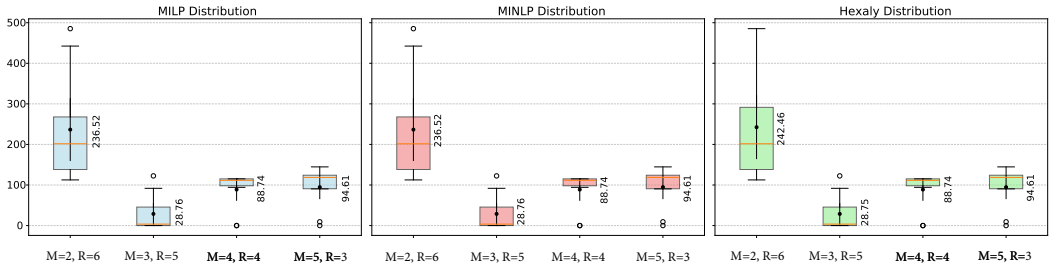

Figure 4. Distribution of objective values across drone-slot configurations (small-sized instances in Riverside).

Table 4. Performance results for small-sized instances in San Bernardino (time in seconds).

Instance				LP		NLP		HX		
County	**Iter**	***M***	***R***	**Obj**	**Time**	**Obj**	**Time**	**Obj**	**Time**	I_q
SB	1	2	6	325.91	166	325.91	300	325.91	300	[30, 570, 30, 570]
SB	2	2	6	292.93	154	292.93	300	292.93	300	[210, 750, 570, 570]
SB	3	2	6	298.20	161	298.20	300	298.20	300	[30, 390, 750, 390]
SB	4	2	6	323.61	300	323.61	300	323.61	300	[30, 390, 390, 30]
SB	5	2	6	453.22	266	453.22	300	453.22	300	[390, 30, 30, 390]
SB	6	2	6	502.27	300	502.27	300	502.27	300	[210, 210, 30, 390]
SB	7	2	6	446.23	300	446.23	300	446.23	300	[30, 210, 210, 570]
SB	8	2	6	631.01	300	631.01	300	631.01	300	[210, 210, 30, 30]
SB	9	2	6	448.45	300	448.45	300	448.45	300	[570, 750, 210, 390]
SB	10	2	6	315.63	199	315.63	300	315.63	300	[390, 930, 210, 750]
SB	1	3	5	121.68	300	121.68	300	121.68	300	[570, 210, 750, 750]
SB	2	3	5	141.25	300	141.25	300	141.25	300	[210, 390, 570, 390]
SB	3	3	5	89.20	175	89.20	300	89.20	300	[30, 570, 750, 390]
SB	4	3	5	136.20	300	136.20	300	136.20	300	[930, 30, 210, 210]
SB	5	3	5	136.42	300	136.42	300	136.42	300	[390, 930, 210, 570]
SB	6	3	5	131.95	262	131.95	300	131.95	300	[30, 210, 210, 390]
SB	7	3	5	123.35	300	123.35	300	123.35	300	[390, 210, 570, 390]
SB	8	3	5	270.54	300	270.54	300	270.54	300	[30, 30, 210, 570]
SB	9	3	5	121.68	300	121.68	300	121.68	300	[750, 570, 210, 390]
SB	10	3	5	127.06	300	127.06	300	127.06	300	[390, 210, 390, 210]
SB	1	4	4	96.80	300	96.80	300	96.80	300	[570, 210, 210, 390]
SB	2	4	4	133.12	300	133.12	300	133.12	300	[30, 390, 210, 30]
SB	3	4	4	123.35	300	123.35	300	123.35	300	[570, 210, 210, 390]
SB	4	4	4	138.58	300	138.58	300	138.58	300	[390, 210, 570, 570]
SB	5	4	4	177.38	300	177.38	300	177.38	300	[210, 390, 210, 390]
SB	6	4	4	127.94	300	127.94	300	127.94	300	[570, 570, 210, 210]
SB	7	4	4	120.54	300	120.54	300	120.54	300	[210, 390, 390, 750]
SB	8	4	4	82.78	100	82.78	300	82.78	300	[30, 570, 210, 570]
SB	9	4	4	0	5	0	11	0	3	[30, 750, 570, 390]
SB	10	4	4	95.76	300	95.76	300	95.76	300	[390, 210, 30, 210]
SB	1	5	3	280.94	300	280.94	300	460.33	300	[210, 930, 30, 30]
SB	2	5	3	0	2	0	4	0	9	[30, 390, 390, 570]
SB	3	5	3	123.35	82	123.35	300	123.35	300	[210, 210, 30, 570]
SB	4	5	3	120.54	25	120.54	151	120.54	300	[30, 570, 1110, 570]
SB	5	5	3	114.03	36	114.03	137	175.72	300	[30, 210, 750, 390]
SB	6	5	3	413.99	208	413.99	300	413.99	300	[30, 210, 210, 30]
SB	7	5	3	280.27	88	280.27	300	280.27	300	[210, 210, 750, 210]
SB	8	5	3	262.78	140	262.78	300	262.78	300	[210, 930, 390, 30]
SB	9	5	3	318.58	38	318.58	300	318.58	300	[210, 210, 390, 210]
SB	10	5	3	246.34	201	246.34	300	246.34	300	[210, 210, 210, 390]

For small-sized instances of the problem, as in Tables 4 and 5, LP and NLP found optimal solutions for all 80 instances. This suggests that, for smaller problem sizes, the problem structure remains tractable under both linear and nonlinear formulations. In addition, HX achieved the same objective values in 74 cases. In six instances, HX returns near-optimal results in the given runtime, possibly due to the increased solution space and the need for additional parameter tuning.

Table 5. Performance results for small-sized instances in Riverside (time in seconds).

Instance				LP		NLP		HX		
County	**Iter**	***M***	***R***	**Obj**	**Time**	**Obj**	**Time**	**Obj**	**Time**	I_q
RS	1	2	6	214.07	60	214.07	300	214.07	300	[570, 390, 570, 570]
RS	2	2	6	185.36	300	185.36	300	185.36	300	[570, 390, 930, 210]
RS	3	2	6	285.04	300	285.04	300	305.98	300	[210, 30, 210, 390]
RS	4	2	6	485.36	300	485.36	300	485.36	300	[210, 210, 210, 30]
RS	5	2	6	189.10	281	189.10	131	189.10	300	[930, 210, 210, 1110]
RS	6	2	6	122.44	195	122.44	46	122.44	300	[210, 930, 570, 390]
RS	7	2	6	112.53	23	112.53	80	112.53	300	[210, 390, 930, 1110]
RS	8	2	6	442.42	300	442.42	300	449.24	300	[390, 210, 30, 570]
RS	9	2	6	215.96	300	215.96	300	247.68	300	[390, 30, 390, 750]
RS	10	2	6	112.88	300	112.88	300	112.88	300	[930, 390, 390, 30]
RS	1	3	5	0	2	0	3	0	11	[390, 570, 30, 210]
RS	2	3	5	0	2	0	5	0	5	[570, 210, 570, 570]
RS	3	3	5	7.12	17	7.12	300	7.12	300	[570, 30, 390, 390]
RS	4	3	5	0	2	0	4	0	28	[570, 210, 750, 30]
RS	5	3	5	122.44	300	122.44	300	122.44	300	[570, 390, 30, 30]
RS	6	3	5	58.04	199	58.04	300	58.04	300	[570, 30, 210, 930]
RS	7	3	5	8.12	300	8.12	300	8.12	300	[390, 30, 930, 930]
RS	8	3	5	0	1	0	36	0	69	[210, 30, 210, 930]
RS	9	3	5	91.83	300	91.83	300	91.83	300	[570, 210, 390, 30]
RS	10	3	5	0	0	0	4	0	1	[570, 390, 390, 210]
RS	1	4	4	109.73	300	109.73	300	109.73	300	[210, 30, 570, 210]
RS	2	4	4	0	2	0	2	0	0	[750, 750, 210, 570]
RS	3	4	4	94.24	300	94.24	300	94.24	300	[390, 30, 390, 30]
RS	4	4	4	111.14	300	111.14	300	111.14	300	[390, 750, 210, 210]
RS	5	4	4	115.09	300	115.09	300	115.09	300	[30, 30, 1110, 570]
RS	6	4	4	111.93	300	111.93	300	111.93	300	[570, 750, 210, 750]
RS	7	4	4	115.09	300	115.09	300	115.09	300	[210, 390, 390, 30]
RS	8	4	4	115.09	300	115.09	300	115.09	300	[30, 930, 1110, 30]
RS	9	4	4	115.09	300	115.09	300	115.09	300	[390, 210, 30, 750]
RS	10	4	4	0	1	0	4	0	4	[570, 210, 390, 570]
RS	1	5	3	0	0	0	1	0	4	[570, 210, 1110, 750]
RS	2	5	3	91.83	8	91.83	133	91.83	300	[570, 30, 570, 210]
RS	3	5	3	9.27	2	9.27	286	9.27	300	[570, 210, 570, 210]
RS	4	5	3	90.45	5	90.45	300	90.45	300	[390, 750, 750, 390]
RS	5	5	3	125.36	7	125.36	300	125.36	300	[390, 570, 390, 210]
RS	6	5	3	122.44	37	122.44	300	122.44	300	[390, 390, 1110, 1110]
RS	7	5	3	124.59	7	124.59	300	124.59	300	[210, 30, 390, 930]
RS	8	5	3	122.44	300	122.44	300	122.44	300	[750, 390, 30, 570]
RS	9	5	3	115.09	12	115.09	300	115.09	300	[210, 570, 30, 390]
RS	10	5	3	144.64	8	144.64	300	144.64	300	[210, 390, 570, 30]

Figures 3 and 4 demonstrate that configurations with more balanced resources, specifically M = 4, R = 4 in San Bernardino and M = 3, R = 5 in Riverside, yield the lowest median objective values and the least variability over different models/solvers. In contrast, setups with either too few drones or limited time-slot flexibility result in higher objective values and wider spreads, highlighting the problem's sensitivity to resource allocation.

Tables 6 and 7 present the outcomes of our proposed formulations across medium-sized instances, covering both the SB_RS and LA test networks. Across all configurations, LP, NLP, and HX produced the same objective value in 27 instances within the time limit, indicating that these solutions are likely optimal. Overall, the LP formulation yielded the

lowest objective values in most cases, a trend that is also reflected in Figures 5 and 6 across various problem instances. Similarly to before, configurations with balanced drone-slot pairings, such as M = 5, R = 5 in the San Bernardino and Riverside case, consistently produce the lowest median objective values and narrower variability.

Table 6. Performance results for medium-sized instances in San Bernardino and Riverside (time in seconds).

Instance				LP		NLP		HX		
County	**Iter**	***M***	***R***	**Obj**	**Time**	**Obj**	**Time**	**Obj**	**Time**	I_q
SB_RS	1	3	8	140.74	1800	180.00	1800	140.74	1800	[210, 390, 30, 750, 390, 210, 30, 210]
SB_RS	2	3	8	114.44	1800	123.66	1800	104.45	1800	[570, 390, 210, 930, 570, 210, 30, 930]
SB_RS	3	3	8	139.30	1800	139.30	1800	139.30	1800	[1110, 750, 390, 210, 210, 390, 570, 210]
SB_RS	4	3	8	53.36	1800	53.36	1800	53.36	1800	[30, 390, 750, 570, 930, 1110, 570, 390]
SB_RS	5	3	8	143.95	1800	170.89	1800	237.80	1800	[30, 570, 210, 750, 30, 750, 1110, 210]
SB_RS	6	3	8	106.94	1800	113.41	1800	113.41	1800	[210, 570, 390, 570, 570, 1110, 30, 210]
SB_RS	7	3	8	206.34	1800	264.09	1800	157.56	1800	[390, 30, 930, 570, 210, 750, 210, 210]
SB_RS	8	3	8	126.93	1800	125.93	1800	129.13	1800	[390, 750, 1110, 570, 390, 570, 930, 210]
SB_RS	9	3	8	134.63	1800	152.65	1800	160.87	1800	[30, 570, 390, 390, 30, 30, 390, 390]
SB_RS	10	3	8	223.90	1800	257.92	1800	316.65	1800	[30, 210, 930, 30, 210, 30, 30, 390]
SB_RS	1	4	6	102.45	1800	102.45	1800	102.45	1800	[390, 930, 390, 930, 570, 30, 210, 210]
SB_RS	2	4	6	275.55	1800	241.93	1800	313.91	1800	[390, 210, 30, 570, 210, 210, 30, 30]
SB_RS	3	4	6	119.32	1800	119.32	1800	119.32	1800	[1110, 210, 390, 210, 930, 570, 210, 210]
SB_RS	4	4	6	92.94	1800	92.94	1800	92.94	1800	[30, 570, 210, 390, 570, 930, 30, 750]
SB_RS	5	4	6	138.27	1800	135.79	1800	138.27	1800	[30, 210, 210, 390, 750, 390, 750, 390]
SB_RS	6	4	6	123.79	1800	123.79	1800	123.79	1800	[750, 210, 30, 570, 570, 390, 930, 30]
SB_RS	7	4	6	128.47	1800	128.47	1800	128.47	1800	[30, 210, 930, 390, 570, 570, 390, 30]
SB_RS	8	4	6	138.36	1800	138.36	1800	138.36	1800	[390, 390, 30, 390, 210, 390, 30, 390]
SB_RS	9	4	6	273.65	1800	273.65	1800	274.92	1800	[30, 30, 30, 390, 570, 1110, 390, 210]
SB_RS	10	4	6	292.59	1800	292.59	1800	292.59	1800	[30, 570, 210, 750, 30, 30, 30, 30]
SB_RS	1	5	5	128.71	1800	128.71	1800	128.71	1800	[30, 30, 210, 210, 390, 930, 750, 210]
SB_RS	2	5	5	109.74	1800	109.74	1800	110.99	1800	[210, 390, 390, 570, 570, 570, 390, 390]
SB_RS	3	5	5	107.24	1800	107.24	1800	107.24	1800	[30, 750, 390, 390, 930, 570, 750, 750]
SB_RS	4	5	5	125.15	1800	125.15	1800	129.85	1800	[30, 390, 210, 390, 570, 30, 570, 210]
SB_RS	5	5	5	117.72	1800	117.72	1800	117.72	1800	[390, 570, 390, 390, 570, 750, 750, 210]
SB_RS	6	5	5	116.08	1800	116.08	1800	116.08	1800	[210, 930, 30, 390, 390, 210, 750, 750]
SB_RS	7	5	5	115.47	1800	115.47	1800	123.54	1800	[930, 390, 570, 390, 750, 570, 30, 210]
SB_RS	8	5	5	113.41	1800	113.41	1800	113.41	1800	[1110, 750, 30, 570, 750, 570, 30, 750]
SB_RS	9	5	5	117.06	1800	117.06	1800	117.06	1800	[30, 570, 30, 570, 210, 30, 390, 30]
SB_RS	10	5	5	138.81	1800	138.81	1800	288.79	1800	[210, 390, 30, 30, 390, 210, 30, 210]
SB_RS	1	6	4	148.92	1800	148.92	1800	148.92	1800	[750, 210, 210, 390, 210, 390, 930, 210]
SB_RS	2	6	4	176.58	1800	190.22	1800	179.25	1800	[390, 750, 30, 750, 210, 390, 210, 210]
SB_RS	3	6	4	265.42	1800	265.42	1800	265.42	1800	[1110, 210, 570, 390, 570, 30, 390, 210]
SB_RS	4	6	4	244.59	1800	244.59	1800	265.12	1800	[30, 210, 30, 570, 30, 30, 390, 930]
SB_RS	5	6	4	239.07	1800	239.07	1800	239.07	1800	[930, 210, 210, 570, 390, 930, 750, 210]
SB_RS	6	6	4	149.29	1800	149.29	1800	149.29	1800	[210, 390, 750, 390, 390, 390, 390, 30]
SB_RS	7	6	4	293.47	1800	293.47	1800	293.47	1800	[390, 570, 30, 750, 390, 390, 210, 750]
SB_RS	8	6	4	273.50	1800	270.78	1800	273.57	1800	[750, 570, 570, 390, 30, 30, 30, 930]
SB_RS	9	6	4	256.03	1800	256.03	1800	256.03	1800	[930, 390, 570, 210, 570, 570, 30, 570]
SB_RS	10	6	4	380.54	1800	380.54	1800	380.54	1800	[30, 210, 210, 210, 390, 570, 570, 210]

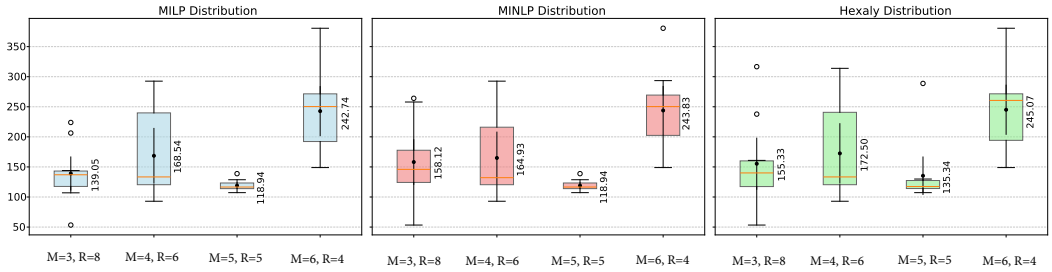

Figure 5. Distribution of objective values across drone-slot configurations (medium-sized instances in San Bernardino and Riverside).

Table 7. Performance results for medium-sized instances in Los Angeles (time in seconds).

Instance				LP		NLP		HX		
County	**Iter**	***M***	***R***	**Obj**	**Time**	**Obj**	**Time**	**Obj**	**Time**	I_q
LA	1	4	8	134.61	3600	126.98	3600	119.08	3600	[390, 210, 210, 570, 750, 210, 210, 210]
LA	2	4	8	98.48	3600	98.48	3600	70.34	3600	[390, 390, 570, 750, 570, 390, 390, 570]
LA	3	4	8	281.37	3600	313.91	3600	329.08	3600	[210, 570, 570, 390, 30, 750, 210, 570]
LA	4	4	8	125.00	3600	137.97	3600	134.29	3600	[390, 390, 390, 30, 570, 390, 570, 570]
LA	5	4	8	207.73	3600	246.22	3600	184.13	3600	[210, 30, 390, 570, 390, 210, 570, 570]
LA	6	4	8	121.32	3600	134.41	3600	134.41	3600	[210, 570, 390, 390, 210, 30, 210, 210]
LA	7	4	8	221.28	3600	171.21	3600	201.80	3600	[390, 750, 390, 570, 210, 390, 390, 30]
LA	8	4	8	370.20	3600	500.59	3600	559.18	3600	[30, 30, 30, 210, 390, 30, 390, 390]
LA	9	4	8	106.03	3600	149.57	3600	131.84	3600	[210, 210, 390, 210, 390, 210, 390, 210]
LA	10	4	8	132.35	3600	180.00	3600	156.97	3600	[570, 210, 210, 210, 210, 570, 30, 390]
LA	1	5	6	363.92	3600	522.94	3600	363.52	3600	[390, 570, 210, 750, 210, 570, 210, 570]
LA	2	5	6	549.14	3600	731.41	3600	657.66	3600	[210, 570, 210, 210, 750, 30, 210, 570]
LA	3	5	6	546.34	3600	548.66	3600	531.71	3600	[390, 390, 210, 390, 570, 390, 30, 570]
LA	4	5	6	510.36	3600	609.51	3600	510.16	3600	[210, 390, 210, 750, 570, 210, 210, 570]
LA	5	5	6	647.48	3600	647.56	3600	647.49	3600	[570, 570, 210, 570, 390, 390, 750, 390]
LA	6	5	6	691.18	3600		3600	666.23	3600	[570, 390, 210, 30, 390, 390, 210, 30]
LA	7	5	6	546.61	3600	1092.91	3600	546.60	3600	[210, 750, 390, 30, 750, 390, 30, 570]
LA	8	5	6	429.00	3600	640.95	3600	467.56	3600	[570, 570, 210, 390, 390, 30, 390, 390]
LA	9	5	6	338.92	3600	374.92	3600	336.52	3600	[570, 750, 570, 390, 570, 570, 390, 750]
LA	10	5	6	331.13	3600	332.18	3600	330.85	3600	[390, 210, 750, 750, 390, 570, 390, 210]
LA	1	5	8	0	775	0	1983	0	335	[210, 210, 390, 390, 390, 750, 390, 390]
LA	2	5	8	258.92	3600	258.92	3600	258.92	3600	[570, 390, 570, 570, 210, 570, 210, 390]
LA	3	5	8	113.80	3600	113.80	3600	113.80	3600	[750, 750, 390, 570, 210, 390, 210, 210]
LA	4	5	8	263.18	3600	263.18	3600	263.18	3600	[30, 390, 210, 390, 390, 210, 570, 210]
LA	5	5	8	116.71	3600	116.71	3600	116.71	3600	[390, 210, 570, 390, 390, 390, 210, 210]
LA	6	5	8	-	3600	-	3600	351.28	3600	[390, 750, 30, 570, 30, 570, 210, 390]
LA	7	5	8	252.42	3600	514.70	3600	154.41	3600	[210, 570, 390, 210, 210, 390, 750, 390]
LA	8	5	8	115.76	3600	115.76	3600	131.78	3600	[390, 210, 210, 750, 210, 210, 390, 570]
LA	9	5	8	115.76	3600	115.76	3600	115.76	3600	[570, 30, 390, 570, 570, 390, 930, 570]
LA	10	5	8	258.92	3600	258.92	3600	258.92	3600	[390, 750, 210, 30, 210, 570, 570, 210]
LA	1	6	5	548.23	3600	577.19	3600	546.68	3600	[390, 390, 390, 30, 390, 750, 390, 390]
LA	2	6	5	510.93	3600	549.11	3600	510.40	3600	[570, 390, 210, 210, 570, 930, 930, 390]
LA	3	6	5	548.99	3600	570.06	3600	547.69	3600	[390, 390, 570, 750, 390, 210, 390, 570]
LA	4	6	5	656.87	3600	629.47	3600	629.47	3600	[210, 210, 570, 390, 570, 570, 930, 210]
LA	5	6	5	691.40	3600	695.97	3600	692.45	3600	[210, 570, 390, 390, 210, 750, 30, 210]
LA	6	6	5	511.34	3600	663.84	3600	510.40	3600	[390, 390, 570, 210, 210, 210, 570, 210]
LA	7	6	5	606.18	3600	690.50	3600	606.16	3600	[570, 390, 570, 390, 210, 570, 390, 390]
LA	8	6	5	723.54	3600	723.69	3600	723.54	3600	[390, 390, 570, 390, 210, 750, 750, 570]
LA	9	6	5	546.60	3600	794.39	3600	546.67	3600	[570, 570, 390, 30, 570, 210, 390, 570]
LA	10	6	5	690.08	3600	690.96	3600	690.08	3600	[390, 390, 390, 390, 210, 570, 750, 390]

Note: "-" under LP and NLP Obj denotes that the models could not find any solutions within 3600 s.

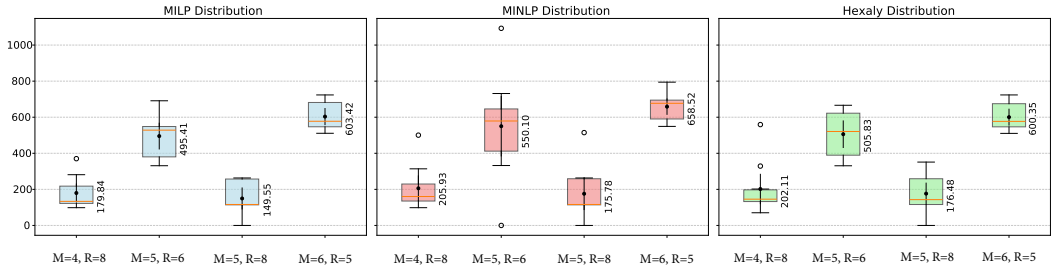

Figure 6. Distribution of objective values across drone-slot configurations (medium-sized instances in Los Angeles).

Table 8. Performance results for large-sized instances in San Bernardino and Los Angeles (time in seconds).

Instance				LP		NLP		HX		
County	**Iter**	***M***	***R***	**Obj**	**Time**	**Obj**	**Time**	**Obj**	**Time**	I_q
SB_LA	1	7	9	114.03	3600	122.17	3600	114.03	3600	[30, 210, 210, 390, 390, 210, 570, 30, 390, 390, 210, 30]
SB_LA	2	7	9	118.86	3600	118.86	3600	118.86	3600	[30, 210, 210, 30, 750, 210, 390, 570, 210, 570, 750, 570]
SB_LA	3	7	9	118.86	3600	155.41	3600	118.86	3600	[750, 30, 570, 30, 390, 390, 390, 390, 210, 390, 390, 210]
SB_LA	4	7	9	114.03	3600	126.09	3600	114.03	3600	[390, 390, 210, 30, 210, 210, 390, 210, 570, 390, 210, 570]
SB_LA	5	7	9	113.80	3600	124.18	3600	113.80	3600	[750, 390, 390, 210, 570, 210, 390, 210, 390, 750, 390, 210]
SB_LA	6	7	9	263.18	3600	337.75	3600	263.18	3600	[750, 390, 390, 570, 210, 570, 570, 390, 570, 210, 390, 210]
SB_LA	7	7	9	118.86	3600	255.33	3600	118.86	3600	[210, 30, 30, 570, 390, 750, 390, 390, 210, 390, 750, 210]
SB_LA	8	7	9	115.76	3600	115.76	3600	115.76	3600	[750, 570, 210, 570, 210, 30, 390, 390, 210, 570, 210, 210]
SB_LA	9	7	9	116.59	3600	116.59	3600	116.59	3600	[930, 750, 570, 210, 210, 210, 570, 750, 210, 390, 390, 210]
SB_LA	10	7	9	0	2444	27.68	3600	0	1483	[390, 390, 210, 570, 210, 390, 210, 570, 210, 390, 570, 570]
SB_LA	1	8	9	258.92	3600	258.91	3600	258.92	3600	[570, 210, 570, 390, 390, 570, 390, 30, 30, 570, 210, 570]
SB_LA	2	8	9	112.32	3600	114.18	3600	112.33	3600	[210, 390, 210, 750, 390, 570, 390, 390, 210, 570, 930, 30]
SB_LA	3	8	9	112.33	3600	112.33	3600	112.33	3600	[930, 750, 390, 750, 390, 210, 390, 390, 390, 390, 390, 30]
SB_LA	4	8	9	114.03	3600	114.03	3600	114.03	3600	[30, 210, 570, 390, 570, 390, 390, 390, 210, 750, 390, 570]
SB_LA	5	8	9	116.71	3600	209.20	3600	116.71	3600	[30, 390, 30, 210, 210, 570, 210, 390, 570, 30, 30, 930]
SB_LA	6	8	9	118.86	3600	278.29	3600	118.86	3600	[570, 30, 930, 570, 570, 930, 390, 570, 210, 210, 570, 210]
SB_LA	7	8	9	263.18	3600	602.53	3600	263.18	3600	[210, 30, 750, 210, 210, 210, 570, 930, 210, 750, 390, 390]
SB_LA	8	8	9	0	1596	246.41	3600	0	613	[570, 750, 210, 210, 390, 570, 390, 570, 210, 210, 210, 750]
SB_LA	9	8	9	115.76	3600	530.65	3600	115.76	3600	[390, 570, 30, 210, 210, 30, 750, 390, 390, 210, 210, 390]
SB_LA	10	8	9	258.92	3600	570.77	3600	258.92	3600	[30, 750, 30, 210, 390, 750, 390, 390, 30, 210, 390, 210]
SB_LA	1	9	8	118.85	3600	118.86	3600	118.86	3600	[390, 210, 210, 210, 210, 30, 390, 570, 570, 210, 750, 750]
SB_LA	2	9	8	258.92	3600	258.92	3600	258.92	3600	[750, 30, 390, 390, 210, 390, 390, 30, 210, 570, 570, 570]
SB_LA	3	9	8	263.18	3600	300.54	3600	263.18	3600	[570, 390, 390, 390, 30, 210, 210, 210, 30, 930, 390, 570]
SB_LA	4	9	8	116.71	3600	116.71	3600	116.71	3600	[210, 210, 210, 390, 390, 210, 210, 390, 210, 210, 390, 30]
SB_LA	5	9	8	114.03	3600	114.03	3600	114.03	3600	[30, 210, 30, 30, 210, 570, 210, 210, 570, 210, 210, 210]
SB_LA	6	9	8	113.80	3600	136.72	3600	113.80	3600	[210, 390, 570, 210, 750, 750, 210, 390, 210, 390, 30, 210]
SB_LA	7	9	8	118.86	3600	118.86	3600	118.86	3600	[390, 30, 210, 570, 390, 390, 570, 30, 210, 390, 390, 30]
SB_LA	8	9	8	107.48	3600	107.48	3600	107.48	3600	[930, 930, 390, 210, 390, 210, 210, 210, 390, 570, 750, 570]
SB_LA	9	9	8	112.33	3600	112.33	3600	112.33	3600	[570, 390, 30, 390, 390, 210, 390, 390, 390, 390, 390, 30]
SB_LA	10	9	8	116.59	3600	116.59	3600	116.59	3600	[750, 750, 930, 570, 390, 930, 210, 390, 390, 210, 570, 390]
SB_LA	1	9	7	116.71	3600	116.71	3600	116.71	3600	[750, 390, 210, 390, 210, 750, 570, 570, 570, 30, 570, 210]
SB_LA	2	9	7	244.96	3600	274.29	3600	244.96	3600	[930, 570, 930, 210, 390, 210, 30, 390, 390, 390, 30, 390]
SB_LA	3	9	7	258.92	3600	258.92	3600	258.92	3600	[570, 210, 930, 390, 390, 750, 390, 390, 210, 210, 30, 210]
SB_LA	4	9	7	116.71	3600	160.93	3600	116.71	3600	[570, 210, 390, 390, 390, 390, 570, 210, 210, 30, 210, 570]
SB_LA	5	9	7	116.59	3600	126.29	3600	116.59	3600	[750, 930, 750, 30, 210, 390, 210, 210, 390, 930, 210, 750]
SB_LA	6	9	7	114.03	3600	114.03	3600	114.03	3600	[30, 210, 30, 30, 390, 570, 210, 390, 570, 210, 210, 930]
SB_LA	7	9	7	258.92	3600	258.92	3600	258.92	3600	[390, 210, 390, 210, 390, 390, 390, 570, 210, 210, 210, 30]
SB_LA	8	9	7	115.75	3600	126.39	3600	115.76	3600	[390, 570, 30, 210, 750, 210, 390, 570, 750, 390, 210, 390]
SB_LA	9	9	7	113.80	3600	113.80	3600	113.80	3600	[30, 750, 1110, 570, 210, 390, 390, 210, 570, 210, 30, 570]
SB_LA	10	9	7	118.86	3600	118.86	3600	118.86	3600	[570, 210, 390, 570, 210, 210, 570, 570, 210, 570, 750, 750]

Tables 8–10 present the results for large-sized instances across San Bernardino, Riverside, and Los Angeles counties. In all 80 instances of the SB_LA and RS_LA test sets, LP and HX produced solutions with identical objective values within the time limit, suggesting that optimal or near-optimal solutions were identified, even at scale. NLP matched these results in 43 instances, showing the complexity of nonlinear routing and battery constraints under tighter visit requirements. Figures 7 and 8 support the findings and indicate that the

M = 9, R = 8 configuration consistently delivers the lowest median objective values and least variability across all solvers.

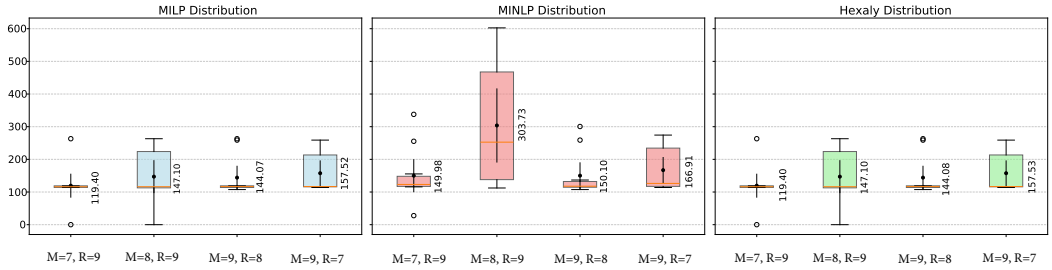

Figure 7. Distribution of objective values across drone-slot configurations (large-sized instances in San Bernardino and Los Angeles).

Table 9. Performance results for large-sized instances in Riverside and Los Angeles (time in seconds).

Instance				LP		NLP		HX		
County	**Iter**	***M***	***R***	**Obj**	**Time**	**Obj**	**Time**	**Obj**	**Time**	I_q
RS_LA	1	7	9	112.33	3600	112.33	3600	112.33	3600	[750, 390, 570, 570, 390, 750, 750, 570, 390, 390, 570, 30]
RS_LA	2	7	9	113.80	3600	-	3600	113.80	3600	[210, 30, 30, 570, 210, 210, 210, 930, 210, 390, 390, 750]
RS_LA	3	7	9	107.48	3600	168.98	3600	107.48	3600	[570, 750, 30, 930, 570, 210, 390, 570, 390, 570, 930, 390]
RS_LA	4	7	9	115.09	3600	115.09	3600	115.09	3600	[210, 390, 210, 390, 570, 390, 570, 210, 390, 390, 210, 750]
RS_LA	5	7	9	116.59	3600	189.38	3600	116.59	3600	[390, 570, 210, 390, 210, 750, 390, 570, 210, 390, 570, 750]
RS_LA	6	7	9	0	1455	141.52	3600	0	1321	[390, 30, 30, 390, 390, 210, 210, 750, 570, 210, 570, 570]
RS_LA	7	7	9	0	1678	325.19	3600	0	462	[210, 390, 210, 930, 390, 390, 210, 390, 570, 390, 750, 390]
RS_LA	8	7	9	115.09	3600	115.09	3600	115.09	3600	[210, 30, 30, 210, 390, 750, 210, 390, 570, 210, 30, 390]
RS_LA	9	7	9	258.92	3600	417.62	3600	258.92	3600	[390, 30, 570, 30, 210, 210, 390, 570, 30, 210, 390, 210]
RS_LA	10	7	9	118.94	3600	682.06	3600	125.32	3600	[30, 930, 750, 210, 210, 390, 210, 30, 210, 750, 210, 750]
RS_LA	1	8	9	116.71	3600	116.71	3600	116.71	3600	[390, 210, 390, 30, 390, 210, 750, 390, 210, 30, 570, 210]
RS_LA	2	8	9	244.96	3600	244.96	3600	244.96	3600	[390, 570, 210, 30, 570, 750, 30, 570, 210, 750, 210, 570]
RS_LA	3	8	9	116.71	3600	116.71	3600	116.71	3600	[30, 750, 210, 1110, 210, 930, 390, 30, 570, 30, 750, 750]
RS_LA	4	8	9	116.71	3600	128.51	3600	116.71	3600	[750, 570, 30, 210, 390, 210, 750, 210, 210, 30, 930, 210]
RS_LA	5	8	9	116.71	3600	314.61	3600	116.71	3600	[570, 390, 930, 210, 210, 390, 390, 390, 210, 210, 30, 390]
RS_LA	6	8	9	263.18	3600	263.18	3600	263.18	3600	[570, 390, 30, 210, 30, 30, 390, 750, 390, 390, 390, 390]
RS_LA	7	8	9	114.46	3600	189.30	3600	114.46	3600	[930, 30, 570, 210, 210, 210, 750, 390, 210, 390, 210, 210]
RS_LA	8	8	9	64.96	3600	64.96	3600	64.96	3600	[570, 1110, 30, 390, 570, 570, 210, 390, 750, 750, 210, 390]
RS_LA	9	8	9	113.80	3600	620.20	3600	113.80	3600	[750, 1110, 30, 210, 570, 750, 390, 390, 210, 390, 390, 570]
RS_LA	10	8	9	114.46	3600	114.46	3600	114.46	3600	[570, 570, 30, 30, 390, 570, 210, 390, 210, 570, 390, 390]
RS_LA	1	9	8	116.59	3600	116.59	3600	116.59	3600	[390, 30, 390, 750, 210, 210, 750, 210, 390, 390, 210, 210]
RS_LA	2	9	8	115.76	3600	115.76	3600	115.76	3600	[570, 570, 30, 30, 390, 30, 210, 210, 390, 210, 390, 390]
RS_LA	3	9	8	115.76	3600	115.76	3600	115.76	3600	[570, 30, 930, 390, 390, 390, 210, 30, 390, 390, 570, 390]
RS_LA	4	9	8	113.80	3600	267.39	3600	113.80	3600	[210, 930, 30, 210, 390, 390, 390, 30, 390, 750, 210, 570]
RS_LA	5	9	8	115.08	3600	200.73	3600	115.09	3600	[390, 210, 210, 930, 390, 210, 210, 750, 210, 570, 570, 570]
RS_LA	6	9	8	112.33	3600	215.59	3600	112.33	3600	[930, 570, 570, 210, 390, 390, 570, 390, 390, 930, 390, 390]
RS_LA	7	9	8	0	744	0	3002	0	653	[390, 30, 210, 570, 390, 210, 570, 210, 390, 750, 930, 210]
RS_LA	8	9	8	116.59	3600	116.59	3600	116.59	3600	[570, 570, 210, 570, 210, 570, 570, 210, 390, 390, 390, 210]
RS_LA	9	9	8	113.43	3600	113.44	3600	113.44	3600	[390, 390, 750, 30, 210, 570, 570, 210, 390, 390, 390, 570]
RS_LA	10	9	8	115.09	3600	115.09	3600	115.09	3600	[30, 390, 390, 390, 390, 750, 210, 570, 390, 750, 570, 210]
RS_LA	1	9	7	112.33	3600	112.33	3600	112.33	3600	[570, 30, 1110, 750, 390, 390, 390, 750, 390, 570, 570, 30]
RS_LA	2	9	7	113.80	3600	118.32	3600	113.80	3600	[390, 210, 30, 570, 210, 390, 390, 210, 390, 750, 30, 930]
RS_LA	3	9	7	244.96	3600	323.01	3600	244.96	3600	[210, 750, 30, 210, 390, 390, 30, 390, 210, 390, 30, 30]
RS_LA	4	9	7	116.71	3600	116.71	3600	116.71	3600	[570, 30, 30, 930, 210, 570, 390, 570, 570, 30, 750, 390]
RS_LA	5	9	7	263.18	3600	263.18	3600	263.18	3600	[390, 210, 30, 570, 30, 210, 390, 570, 210, 210, 210, 30]
RS_LA	6	9	7	115.76	3600	115.76	3600	115.76	3600	[210, 30, 930, 210, 390, 30, 570, 390, 210, 570, 30, 570]
RS_LA	7	9	7	115.76	3600	115.76	3600	115.76	3600	[390, 750, 390, 750, 570, 30, 390, 210, 390, 930, 570, 390]
RS_LA	8	9	7	113.44	3600	113.44	3600	113.44	3600	[750, 210, 390, 570, 390, 210, 390, 210, 390, 390, 210, 930]
RS_LA	9	9	7	115.76	3600	115.76	3600	115.76	3600	[210, 390, 570, 210, 210, 210, 390, 210, 390, 390, 210, 570]
RS_LA	10	9	7	113.44	3600	113.44	3600	113.44	3600	[210, 210, 210, 750, 390, 210, 390, 210, 210, 390, 570, 750]

Note: "-" under NLP Obj denotes that NLP could not find any solutions within 3600 s.

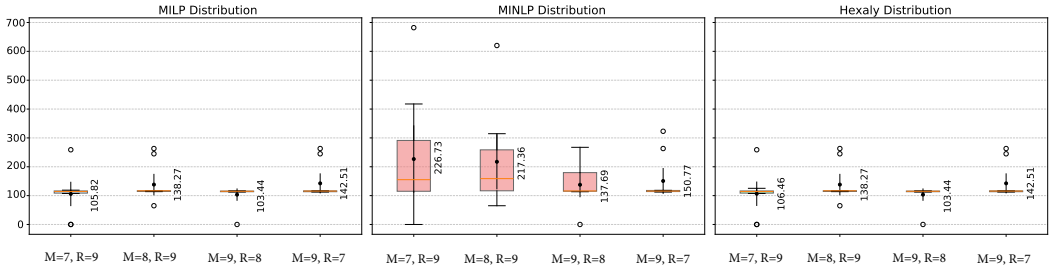

Figure 8. Distribution of objective values across drone-slot configurations (large-sized instances in Riverside and Los Angeles).

Table 10. Performance results for large-sized instances in San Bernardino, Riverside, and Los Angeles (time in seconds).

Instance				LP		NLP		HX		
County	**Iter**	***M***	***R***	**Obj**	**Time**	**Obj**	**Time**	**Obj**	**Time**	I_q
SB_RS_LA	1	8	7	277.18	3600	-	3600	244.96	3600	[390, 30, 30, 210, 570, 750, 570, 390, 390, 570, 30, 210, 390, 750, 570, 390]
SB_RS_LA	2	8	7	266.69	3600	-	3600	121.29	3600	[390, 390, 30, 570, 210, 390, 570, 750, 210, 570, 210, 210, 570, 570, 390, 570]
SB_RS_LA	3	8	7	439.27	3600	-	3600	189.54	3600	[30, 210, 30, 570, 30, 30, 570, 210, 210, 930, 390, 210, 390, 570, 210, 30]
SB_RS_LA	4	8	7	313.14	3600	1008.33	3600	258.92	3600	[570, 30, 930, 390, 750, 930, 210, 570, 390, 390, 570, 30, 210, 750, 570, 390]
SB_RS_LA	5	8	7	441.69	3600	-	3600	120.09	3600	[210, 30, 390, 930, 390, 210, 30, 930, 210, 30, 390, 750, 210, 930, 750, 210]
SB_RS_LA	6	8	7	353.18	3600	-	3600	120.63	3600	[930, 750, 30, 390, 570, 750, 30, 210, 210, 30, 210, 750, 570, 390, 390, 570]
SB_RS_LA	7	8	7	417.74	3600	-	3600	126.80	3600	[210, 750, 570, 30, 390, 930, 570, 390, 210, 570, 210, 210, 570, 210, 390, 570]
SB_RS_LA	8	8	7	653.29	3600	927.47	3600	285.95	3600	[30, 30, 750, 390, 750, 210, 570, 30, 30, 210, 30, 390, 390, 210, 210, 210]
SB_RS_LA	9	8	7	398.61	3600	-	3600	258.92	3600	[390, 570, 1110, 570, 570, 30, 30, 390, 390, 570, 390, 210, 30, 210, 570, 390]
SB_RS_LA	10	8	7	356.08	3600	1058.75	3600	117.37	3600	[210, 570, 30, 30, 390, 750, 30, 750, 210, 570, 570, 390, 390, 210, 210, 390]
SB_RS_LA	1	8	9	338.37	3600	-	3600	263.18	3600	[570, 210, 390, 210, 30, 930, 390, 930, 210, 210, 210, 390, 570, 390, 390, 210]
SB_RS_LA	2	8	9	278.37	3600	708.87	3600	258.92	3600	[390, 210, 390, 390, 210, 210, 210, 570, 210, 750, 210, 570, 30, 750, 750, 390]
SB_RS_LA	3	8	9	116.71	3600	415.16	3600	116.71	3600	[210, 570, 570, 570, 390, 570, 570, 570, 210, 210, 390, 210, 390, 30, 570, 750]
SB_RS_LA	4	8	9	114.03	3600	-	3600	114.03	3600	[30, 210, 210, 30, 570, 30, 210, 390, 210, 750, 390, 570, 390, 750, 750, 390]
SB_RS_LA	5	8	9	172.39	3600	-	3600	115.09	3600	[390, 210, 390, 210, 210, 390, 30, 210, 390, 390, 210, 390, 570, 750, 210, 570]
SB_RS_LA	6	8	9	310.95	3600	1106.08	3600	124.75	3600	[30, 390, 30, 210, 390, 570, 210, 210, 210, 30, 750, 210, 570, 210, 210, 570]
SB_RS_LA	7	8	9	254.08	3600	-	3600	118.86	3600	[30, 390, 210, 390, 390, 570, 570, 750, 210, 570, 750, 30, 570, 390, 210, 210]
SB_RS_LA	8	8	9	252.48	3600	-	3600	118.86	3600	[210, 30, 390, 570, 390, 30, 30, 30, 210, 210, 210, 390, 750, 210, 390, 390]
SB_RS_LA	9	8	9	331.03	3600	-	3600	115.76	3600	[390, 390, 30, 570, 390, 30, 930, 390, 570, 30, 390, 570, 210, 930, 390, 210]
SB_RS_LA	10	8	9	263.18	3600	-	3600	263.18	3600	[570, 570, 390, 390, 570, 390, 210, 930, 30, 570, 390, 210, 210, 390, 210, 930]
SB_RS_LA	1	9	7	103.54	3600	596.03	3600	102.70	3600	[30, 750, 30, 390, 390, 570, 390, 750, 390, 210, 390, 390, 210, 750, 570, 750]
SB_RS_LA	2	9	7	268.83	3600	-	3600	263.18	3600	[930, 750, 390, 390, 210, 570, 390, 30, 210, 390, 210, 210, 390, 390, 30, 210]
SB_RS_LA	3	9	7	135.02	3600	-	3600	112.33	3600	[1110, 210, 750, 750, 210, 210, 930, 30, 570, 390, 390, 570, 210, 570, 390, 30]
SB_RS_LA	4	9	7	263.18	3600	-	3600	263.18	3600	[30, 570, 750, 570, 390, 30, 210, 210, 30, 390, 390, 210, 390, 390, 390, 570]
SB_RS_LA	5	9	7	231.01	3600	825.48	3600	124.00	3600	[1110, 210, 750, 390, 30, 570, 930, 390, 390, 30, 570, 210, 390, 570, 570, 30]
SB_RS_LA	6	9	7	118.86	3600	352.47	3600	118.86	3600	[570, 210, 390, 390, 570, 210, 390, 570, 390, 930, 390, 390, 390, 570, 390, 570]
SB_RS_LA	7	9	7	244.96	3600	-	3600	244.96	3600	[210, 570, 390, 750, 210, 210, 570, 570, 210, 750, 30, 390, 390, 570, 570, 390]
SB_RS_LA	8	9	7	85.12	3600	811.11	3600	28.38	3600	[210, 390, 570, 570, 210, 210, 390, 30, 570, 390, 390, 390, 570, 570, 210, 570]
SB_RS_LA	9	9	7	219.11	3600	766.65	3600	116.59	3600	[750, 570, 570, 570, 390, 1110, 30, 570, 210, 570, 210, 570, 390, 570, 210, 570]
SB_RS_LA	10	9	7	221.60	3600	-	3600	116.59	3600	[30, 390, 570, 210, 390, 210, 930, 390, 210, 390, 390, 570, 390, 570, 30, 390]
SB_RS_LA	1	9	8	388.62	3600	-	3600	122.45	3600	[30, 570, 210, 210, 30, 30, 390, 390, 210, 210, 210, 30, 210, 210, 750, 210]
SB_RS_LA	2	9	8	238.78	3600	-	3600	119.74	3600	[210, 210, 30, 570, 210, 570, 30, 30, 390, 750, 210, 30, 570, 210, 390, 30]
SB_RS_LA	3	9	8	113.44	3600	272.46	3600	113.44	3600	[210, 570, 30, 570, 570, 390, 30, 930, 390, 570, 570, 30, 390, 750, 210, 750]
SB_RS_LA	4	9	8	317.44	3600	-	3600	131.50	3600	[210, 930, 570, 30, 210, 30, 390, 930, 210, 750, 570, 30, 390, 30, 390, 210]
SB_RS_LA	5	9	8	200.97	3600	-	3600	113.44	3600	[30, 210, 390, 570, 570, 30, 210, 210, 570, 570, 210, 210, 390, 210, 210, 570]
SB_RS_LA	6	9	8	159.84	3600	1101.55	3600	116.71	3600	[390, 390, 30, 390, 30, 750, 390, 1110, 570, 30, 210, 750, 570, 30, 390, 210]
SB_RS_LA	7	9	8	174.31	3600	507.07	3600	113.80	3600	[750, 210, 390, 570, 570, 210, 30, 750, 390, 390, 750, 390, 210, 210, 210, 570]
SB_RS_LA	8	9	8	184.13	3600	765.34	3600	115.76	3600	[750, 750, 210, 210, 210, 210, 930, 390, 390, 30, 390, 30, 390, 210, 390, 570]
SB_RS_LA	9	9	8	112.33	3600	335.99	3600	112.33	3600	[390, 390, 210, 570, 390, 750, 30, 210, 210, 750, 210, 570, 570, 390, 570, 30]
SB_RS_LA	10	9	8	116.71	3600	-	3600	116.71	3600	[390, 750, 1110, 930, 750, 210, 30, 210, 570, 750, 210, 570, 390, 210, 570, 570]

Note: "-" under NLP Obj denotes that NLP could not find any solutions within 3600 s.

Table 10 shows that both LP and NLP were unable to guarantee optimal solutions for the largest problem instances within the time limit. This outcome is expected, given the NP-hard nature of the problem and the rapid growth in complexity as the number of targets, drones, and time slots increases. The NLP formulation produced feasible solutions for only 16 out of the 40 largest instances, with noticeably higher objective values than those obtained by HX. In contrast, the LP model returned feasible solutions for all 40 instances, and, in 9 of them, its objective value exactly matched the best HX solution.

One of the key factors influencing solver behavior is the inter-visit time parameter I_q. The results over all cases show that configurations with heterogeneous or tightly bound I_q values lead to higher objective values and increased computational effort, par-

ticularly for NLP and HX. This reinforces the role of I_q as a core design lever in drone scheduling systems.

Figure 9 shows that, for all models/solvers, the M = 9, R = 8 configuration produces the lowest median objective values with the least variability. HX outperforms both LP and NLP in terms of median objective value and stability, which indicates its effectiveness for complex large-scale scenarios.

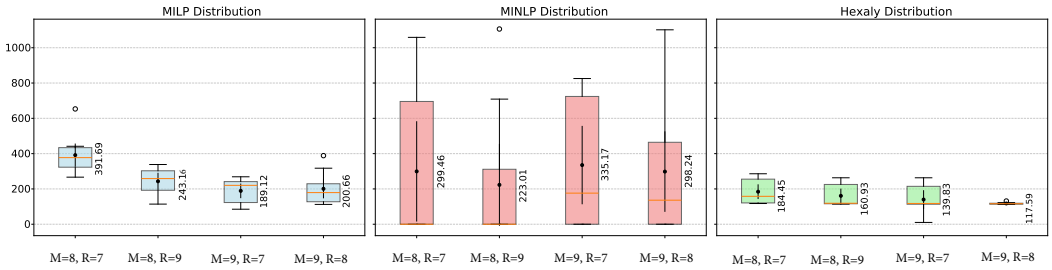

Figure 9. Distribution of objective values across drone-slot configurations (large-sized instances in San Bernardino, Riverside, and Los Angeles).

Figures 10 and 11 show the convergence profiles of the LP, NLP, and HX, especially for the large-sized instances.

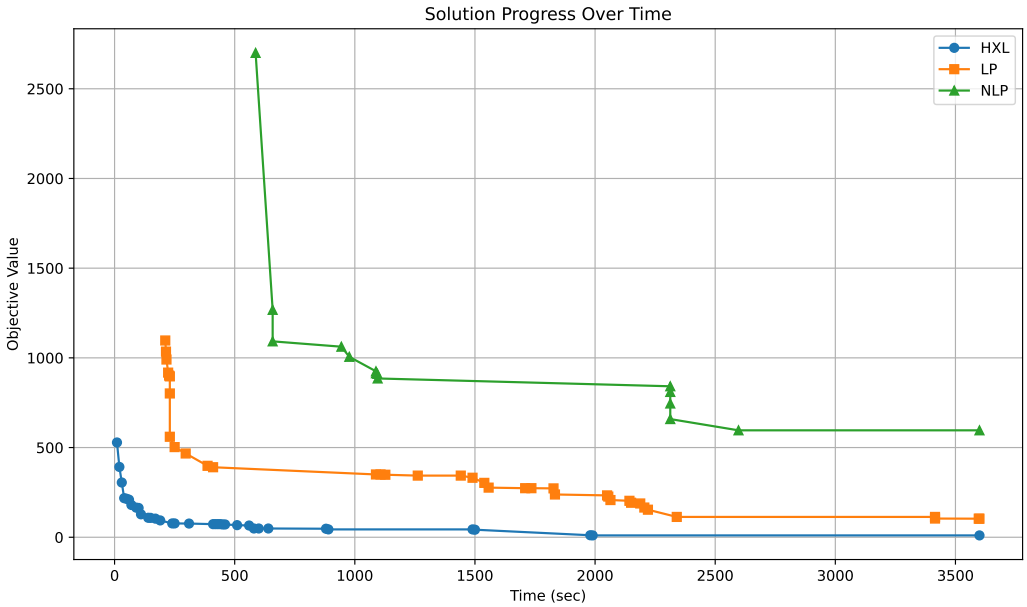

Figure 10. Comparing the convergence profile of LP, NLP, and HX for SB_RS_LA iteration 1 instance with 9 drones and 7 slots.

Figures 10 and 11 reveal both the speed with which the models/solvers locate a first feasible solution and the quality of the improvements that they can secure before the time limit. HX reaches a feasible solution almost immediately and converges efficiently, which shows the typical speed advantage of a heuristic. LP improves steadily, but much more slowly, while NLP struggles to escape suboptimal regions and has modest progress. This is due to the fragmented solution space of the DRSFMV problem, caused by tight inter-visit constraints, battery limits, and slot-based scheduling, which leads to a non-convex and discontinuous feasible region. Small changes in decision variables can easily break feasibility, making the problem especially hard for exact methods. HX, by contrast, is better equipped to explore disconnected regions to deliver high-quality results under complex, large-scale scenarios.

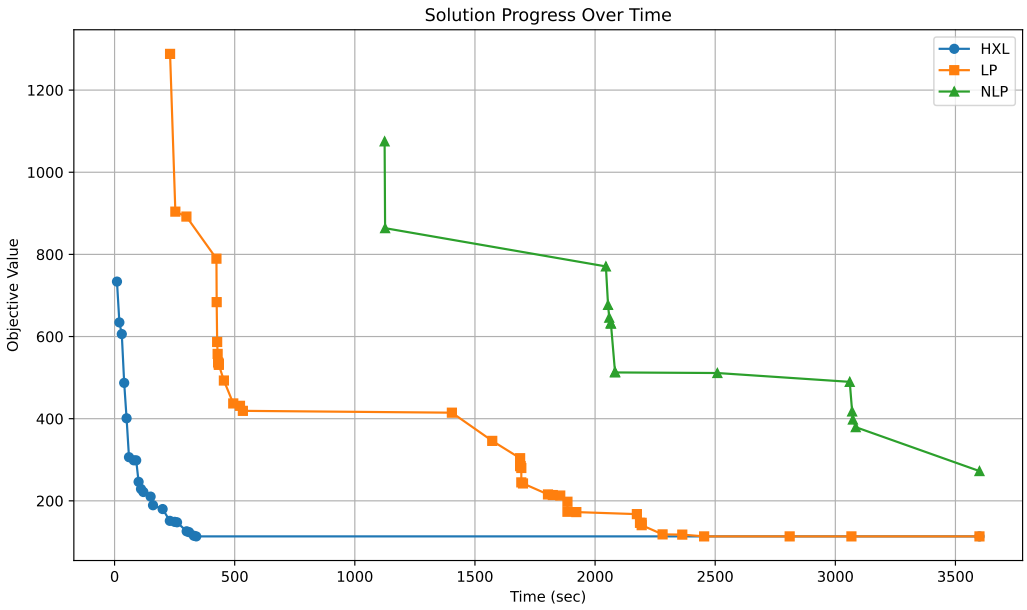

Figure 11. Comparing the convergence profile of LP, NLP, and HX for SB_RS_LA iteration 3 instance with 9 drones and 8 slots.

5. Conclusions

Compared to traditional traffic monitoring methods such as police patrols, fixed cameras, or helicopters, which are often costly, labor-intensive, and limited in coverage, drones offer a more flexible, cost-effective, and environmentally friendly alternative. They enable the dynamic coverage of high-risk areas, reduce response time to incidents, and can be deployed even in resource-constrained environments. This paper introduced the Drone Routing and Scheduling with Flexible Multiple Visits (DRSFMV) problem for highway traffic monitoring. A mixed-integer nonlinear programming (MINLP) model and its linearized version (MILP) are developed to schedule drones that repeatedly monitor critical road segments under constraints such as battery limits, variable monitoring durations, recharging needs, and inter-visit time limits. The model aims to minimize the maximum lateness and earliness of visits while ensuring continuous and efficient coverage. The problem was also implemented using Hexaly (HX), a heuristic-based solver, to address the increasing complexity as the problem size grows. Using real traffic data from highways in San Bernardino, Riverside, and Los Angeles counties in Southern California, the models and solvers were tested on small, medium, and large instances. Across 120 total instances of varying size and complexity, the LP solver returned optimal or feasible solutions in 119 cases, while NLP succeeded in only 93 instances. HX achieved 100% feasibility and matched or improved upon LP solutions in most instances, especially for large-scale cases. The sensitivity analysis highlights important trade-offs between the number of drones and slot flexibility, indicating that balanced resource pairs minimize objective function value and variability.

A limitation of this study includes the use of identical drones, one depot, and deterministic travel times. Future studies could explore more realistic settings with multiple depots, different drone types, and uncertain traffic conditions. Another limitation is the absence of real-world implementation data to validate the proposed drone routing and scheduling model. Although the experiments are based on real traffic census data and reflect practical operational constraints, there are currently no publicly available datasets that capture detailed drone routing and scheduling behavior in traffic monitoring applications. Existing datasets mainly provide vehicle trajectory data recorded by drones, but

do not include information on the drones' own operations, such as flight paths, battery usage, or scheduling decisions. As a future direction, conducting a real-world case study in collaboration with transportation or public safety agencies would be highly valuable. This would help benchmark the model under practical conditions and offer valuable feedback for refining the framework to support real-world applications.

Author Contributions: Conceptualization, N.M.-K. and S.A.; methodology, N.M.-K., S.A. and O.T.; software, N.M.-K. and O.T.; validation, N.M.-K., S.A. and O.T.; formal analysis, N.M.-K., S.A. and O.T.; writing—original draft preparation, N.M.-K., S.A. and O.T.; writing—review and editing, N.M.-K., S.A. and O.T.; visualization, O.T.; supervision, N.M.-K. and O.T. All authors have read and agreed to the published version of the manuscript.

Funding: This research received no external funding.

Data Availability Statement: All the implementation codes and the results are available online on the Github address: https://github.com/oguztoragay/DRONES (accessed on 25 July 2025).

Acknowledgments: This work was supported in part by the High-Performance Computing Program at California State University San Bernardino (CSUSB); NSF awards CNS-1730158, ACI-1540112, ACI-1541349, OAC-1826967, OAC-2112167, CNS-2120019; the University of California Office of the President; and the University of California San Diego's California Institute for Telecommunications and Information Technology/Qualcomm Institute. The authors would like to thank Youngsu Kim and Dung Vu at CSUSB for their valuable assistance and technical support in configuring and utilizing the HPC resources for this research.

Conflicts of Interest: The authors declare no conflicts of interest.

References

1. National Highway Traffic Safety Administration. Overview of Motor Vehicle Traffic Crashes in 2022. 2024. Available online: https://rosap.ntl.bts.gov/view/dot/78044 (accessed on 20 May 2025).
2. Abdelkader, G.; Elgazzar, K.; Khamis, A. Connected vehicles: Technology review, state of the art, challenges and opportunities. *Sensors* **2021**, *21*, 7712. [CrossRef] [PubMed]
3. Office of the City Controller, City of Los Angeles. Audit of the Los Angeles Police Department's Air Support Division in 2023. Available online: https://controller.lacity.gov/landings/lapd-helicopters (accessed on 5 July 2025).
4. Public Policy Institute of California. Law Enforcement Staffing in California. PPIC Fact Sheet, February 2025. Available online: https://www.ppic.org/publication/law-enforcement-staffing-in-california/ (accessed on 25 June 2025).
5. Wu, X.; Lum, C.; Koper, C. Do everyday proactive policing activities reduce vehicle crashes? examining a commonly held law enforcement belief using a novel method. *J. Crim. Justice* **2021**, *76*, 101846. [CrossRef]
6. U.S. Department of Transportation, Federal Highway Administration. Common Issues in Emergency Transportation Operations Preparedness and Response: Results of the FHWA Workshop Series FHWA Office of Operations. Available online: https://rosap.ntl.bts.gov/view/dot/20659 (accessed on 4 May 2025).
7. Mohabbati-Kalejahi, N.; Vinel, A. Robust hazardous materials closed-loop supply chain network design with emergency response teams location. *Transp. Res. Rec.* **2021**, *2675*, 306–329. [CrossRef]
8. Coifman, B.; McCord, M.; Mishalani, R.G.; Iswalt, M.; Ji, Y. Roadway traffic monitoring from an unmanned aerial vehicle. *IEE Proc.—Intell. Transp. Syst.* **2006**, *153*, 11–20. [CrossRef]
9. McCormack, E.D. *The Use of Small Unmanned Aircraft by the Washington State Department of Transportation*; Technical Report WA-RD 703.1; Washington State Dept. of Transportation: Olympia, WA, USA, 2008.
10. Zhang, X.; Guan, Z.; Liu, X.; Zhang, Z. Digital reconstruction method for low-illumination road traffic accident scenes using uav and auxiliary equipment. *World Electr. Veh. J.* **2025**, *16*, 171. [CrossRef]
11. Malveaux, C.; de Queiroz, M.; Li, X.; Hassan, H.; He, Z. *Real-Time Work Zone Traffic Management via Unmanned Air Vehicles*; Technical Report; Louisiana State University Transportation Research Center: Baton Rouge, LA, USA, 2020.
12. Askarzadeh, T.; Bridgelall, R.; Tolliver, D. Drones for road condition monitoring: Applications and benefits. *J. Transp. Eng. Part B Pavements* **2023**, *151*, 04024055. [CrossRef]
13. Roldán, J.J.; Joossen, G.; Sanz, D.; del Cerro, J.; Barrientos, A. Mini-uav based sensory system for measuring environmental variables in greenhouses. *Sensors* **2015**, *15*, 3334–3350. [CrossRef]

14. Villa, T.F.; Salimi, F.; Morton, K.; Morawska, L.; Gonzalez, F. Development and validation of a uav based system for air pollution measurements. *Sensors* **2016**, *16*, 2202. [CrossRef]
15. Pasha, J.; Elmi, Z.; Purkayastha, S.; Fathollahi-Fard, A.M.; Ge, Y.-E.; Lau, Y.-Y.; Dulebenets, M.A. The drone scheduling problem: A systematic state-of-the-art review. *IEEE Trans. Intell. Transp. Syst.* **2022**, *23*, 14224–14247. [CrossRef]
16. Glock, K.; Meyer, A. Mission planning for emergency rapid mapping with drones. *Transp. Sci.* **2020**, *54*, 534–560. [CrossRef]
17. Akram, T.; Awais, M.; Naqvi, R.; Ahmed, A.; Naeem, M. Multicriteria uav base stations placement for disaster management. *IEEE Syst. J.* **2020**, *14*, 3475–3482. [CrossRef]
18. Banik, D.; Hossain, N.U.I.; Govindan, K.; Nur, F.; Babski-Reeves, K. A decision support model for selecting unmanned aerial vehicle for medical supplies: Context of covid-19 pandemic. *Int. J. Logist. Manag.* **2023**, *34*, 473–496. [CrossRef]
19. Huang, H.; Savkin, A.V.; Huang, C. Scheduling of a parcel delivery system consisting of an aerial drone interacting with public transportation vehicles. *Sensors* **2020**, *20*, 2045. [CrossRef]
20. Shi, Y.; Lin, Y.; Li, B.; Li, R.Y.M. A bi-objective optimization model for the medical supplies' simultaneous pickup and delivery with drones. *Comput. Ind. Eng.* **2022**, *171*, 108389. [CrossRef]
21. Cheema, M.A.; Ansari, R.I.; Ashraf, N.; Hassan, S.A.; Qureshi, H.K.; Bashir, A.K.; Politis, C. Blockchain-based secure delivery of medical supplies using drones. *Comput. Netw.* **2022**, *204*, 108706. [CrossRef]
22. Li, M.; Zhen, L.; Wang, S.; Lv, W.; Qu, X. Unmanned aerial vehicle scheduling problem for traffic monitoring. *Comput. Ind. Eng.* **2018**, *122*, 15–23. [CrossRef]
23. Khan, M.A.; Ectors, W.; Bellemans, T.; Janssens, D.; Wets, G. Uav-based traffic analysis: A universal guiding framework based on literature survey. *Transp. Res. Procedia* **2017**, *22*, 541–550. [CrossRef]
24. Elloumi, M.; Dhaou, R.; Escrig, B.; Idoudi, H.; Saidane, L.A. Monitoring road traffic with a uav-based system. In Proceedings of the 2018 IEEE Wireless Communications and Networking Conference (WCNC), Barcelona, Spain, 15–18 April 2018; IEEE: Piscataway, NJ, USA, 2018; pp. 1–6.
25. Barmpounakis, E.; Geroliminis, N. On the new era of urban traffic monitoring with massive drone data: The pneuma large-scale field experiment. *Transp. Res. Part C Emerg. Technol.* **2020**, *111*, 50–71. [CrossRef]
26. Outay, F.; Mengash, H.A.; Adnan, M. Applications of unmanned aerial vehicle (uav) in road safety, traffic and highway infrastructure management: Recent advances and challenges. *Transp. Res. Part A Policy Pract.* **2020**, *141*, 116–129. [CrossRef]
27. Khan, N.A.; Jhanjhi, N.Z.; Brohi, S.N.; Usmani, R.S.A.; Nayyar, A. Smart traffic monitoring system using unmanned aerial vehicles (uavs). *Comput. Commun.* **2020**, *157*, 434–443. [CrossRef]
28. Ahmed, A.; Outay, F.; Zaidi, S.O.R.; Adnan, M.; Ngoduy, D. Examining queue-jumping phenomenon in heterogeneous traffic stream at signalized intersection using uav-based data. *Pers. Ubiquitous Comput.* **2021**, *25*, 93–108. [CrossRef]
29. Beg, A.; Qureshi, A.R.; Sheltami, T.; Yasar, A. Uav-enabled intelligent traffic policing and emergency response handling system for the smart city. *Pers. Ubiquitous Comput.* **2021**, *25*, 33–50. [CrossRef]
30. Kumar, A.; Yadav, A.S.; Gill, S.S.; Pervaiz, H.; Ni, Q.; Buyya, R. A secure drone-to-drone communication and software defined drone network-enabled traffic monitoring system. *Simul. Model. Pract. Theory* **2022**, *120*, 102621. [CrossRef]
31. Kainz, O.; Dopiriak, M.; Michalko, M.; Jakab, F.; Nováková, I. Traffic monitoring from the perspective of an unmanned aerial vehicle. *Appl. Sci.* **2022**, *12*, 7966. [CrossRef]
32. Butilă, E.V.; Boboc, R.G. Urban traffic monitoring and analysis using unmanned aerial vehicles (uavs): A systematic literature review. *Remote Sens.* **2022**, *14*, 620. [CrossRef]
33. Bisio, I.; Garibotto, C.; Haleem, H.; Lavagetto, F.; Sciarrone, A. A systematic review of drone based road traffic monitoring system. *IEEE Access* **2022**, *10*, 101537–101555. [CrossRef]
34. Fan, M.; Wu, Y.; Liao, T.; Cao, Z.; Guo, H.; Sartoretti, G.; Wu, G. Deep reinforcement learning for uav routing in the presence of multiple charging stations. *IEEE Trans. Veh. Technol.* **2022**, *72*, 5732–5746. [CrossRef]
35. Chow, J.Y.J. Dynamic uav-based traffic monitoring under uncertainty as a stochastic arc-inventory routing policy. *Int. J. Transp. Sci. Technol.* **2016**, *5*, 167–185. [CrossRef]
36. Luo, Z.; Liu, Z.; Shi, J. A two-echelon cooperated routing problem for a ground vehicle and its carried unmanned aerial vehicle. *Sensors* **2017**, *17*, 1144. [CrossRef]
37. Hu, M.; Liu, W.; Peng, K.; Ma, X.; Cheng, W.; Liu, J. Joint routing and scheduling for vehicle-assisted multidrone surveillance. *IEEE Internet Things J.* **2018**, *6*, 1781–1790. [CrossRef]
38. Luo, H.; Zhang, P.; Wang, J.; Wang, G.; Meng, F. Traffic patrolling routing problem with drones in an urban road system. *Sensors* **2019**, *19*, 5164. [CrossRef]
39. Xu, B.; Zhao, K.; Luo, Q.; Wu, G.; Pedrycz, W. A gv-drone arc routing approach for urban traffic patrol by coordinating a ground vehicle and multiple drones. *Swarm Evol. Comput.* **2023**, *77*, 101246. [CrossRef]
40. Zhang, J.; Jia, L.; Niu, S.; Zhang, F.; Tong, L.; Zhou, X. A space-time network-based modeling framework for dynamic unmanned aerial vehicle routing in traffic incident monitoring applications. *Sensors* **2015**, *15*, 13874–13898. [CrossRef]

41. Ghazzai, H.; Kadri, A.; Ghorbel, B.; Menouar, H.; Massoud, Y. A generic spatiotemporal uav scheduling framework for multi-event applications. *IEEE Access* **2018**, *7*, 215–229. [CrossRef]
42. Ghazzai, H.; Menouar, H.; Kadri, A.; Massoud, Y. Future uav-based its: A comprehensive scheduling framework. *IEEE Access* **2019**, *7*, 75678–75695. [CrossRef]
43. Christodoulou, C.; Kolios, P. Optimized tour planning for drone-based urban traffic monitoring. In Proceedings of the 2020 IEEE 91st Vehicular Technology Conference (VTC2020-Spring), Antwerp, Belgium, 25–28 May 2020; IEEE: Piscataway, NJ, USA, 2020; pp. 1–5.
44. Kumar, A.; Krishnamurthi, R.; Nayyar, A.; Luhach, A.K.; Khan, M.S.; Singh, A. A novel software-defined drone network (sddn)-based collision avoidance strategies for on-road traffic monitoring and management. *Veh. Commun.* **2021**, *28*, 100313. [CrossRef]
45. Rigas, E.S.; Kolios, P.; Mavrovouniotis, M.; Ellinas, G. Scheduling a fleet of drones for monitoring missions with spatial, temporal, and energy constraints. *IEEE Trans. Intell. Transp. Syst.* **2021**, *23*, 15133–15145. [CrossRef]
46. Yakıcı, E. Solving location and routing problem for uavs. *Comput. Ind. Eng.* **2016**, *102*, 294–301. [CrossRef]
47. Terzi, M.; Kolios, P.; Panayiotou, C.; Theocharides, T. A unified framework for reliable multi-drone tasking in emergency response missions. In Proceedings of the 2019 International Conference on Unmanned Aircraft Systems (ICUAS), Atlanta, GA, USA, 11–14 June 2019; IEEE: Piscataway, NJ, USA, 2019; pp. 819–827.
48. Oh, H.; Kim, S.; Tsourdos, A.; White, B.A. Coordinated road-network search route planning by a team of uavs. *Int. J. Syst. Sci.* **2014**, *45*, 825–840. [CrossRef]
49. Campbell, J.F.; Corberán, Á.; Plana, I.; Sanchis, J.M.; Segura, P. Solving the length constrained k-drones rural postman problem. *Eur. J. Oper. Res.* **2021**, *292*, 60–72. [CrossRef]
50. Wang, K.; Wu, Q.; He, X.; Hu, C.; Chen, N. Optimizing uav traffic monitoring routes during rush hours considering spatiotemporal variation of monitoring demand. *Int. J. Geogr. Inf. Sci.* **2022**, *36*, 2086–2111. [CrossRef]
51. Cheng, L.; Zhong, L.; Tian, S.; Xing, J. Task assignment algorithm for road patrol by multiple uavs with multiple bases and rechargeable endurance. *IEEE Access* **2019**, *7*, 144381–144397. [CrossRef]
52. Huang, H.; Savkin, A.V.; Huang, C. Decentralized autonomous navigation of a uav network for road traffic monitoring. *IEEE Trans. Aerosp. Electron. Syst.* **2021**, *57*, 2558–2564. [CrossRef]
53. Niu, S.; Zhang, J.; Zhang, F.; Li, H. A method of uavs route optimization based on the structure of the highway network. *Int. J. Distrib. Sens. Netw.* **2015**, *11*, 359657. [CrossRef]
54. Jo, J.-M. Highway drone patrol network topology and performance analysis for traffic violation enforcement. *J. Korean Inst. Electron. Commun.* **2017**, *12*, 1043–1048.
55. Li, J.; Cao, X.; Guo, D.; Xie, J.; Chen, H. Task scheduling with uav-assisted vehicular cloud for road detection in highway scenario. *IEEE Internet Things J.* **2020**, *7*, 7702–7713. [CrossRef]
56. Kim, S.; Jin, Y.; Jeong, B.; Han, J. Models and case studies for optimal deployment and scheduling of highway surveillance drones. *Korean Manag. Sci. Rev.* **2022**, *39*, 29–41. [CrossRef]
57. Choi, S.; Lee, M.; Park, H.; Han, J. Mathematical programming-based heuristic for highway patrol drone scheduling problem. *Socio-Econ. Plan. Sci.* **2024**, *93*, 101907. [CrossRef]
58. Bérczi, K.; Mnich, M.; Vincze, R. Approximations for many-visits multiple traveling salesman problems. *Omega* **2023**, *116*, 102816. [CrossRef]
59. California Department of Transportation. Truck Traffic: Annual Average Daily Truck Traffic. 2020. Available online: https://gisdata-caltrans.opendata.arcgis.com/search?tags=Highway (accessed on 21 October 2024).
60. Sandia National Laboratories. *Pyomo: Python Optimization Modeling Objects*, Version 6.7.0; Sandia National Laboratories: Albuquerque, NM, USA, 2023. Available online: https://github.com/Pyomo/pyomo (accessed on 7 February 2025).
61. LLC Gurobi Optimization. Gurobi Optimizer Version 12.0.1 Reference Manual. 2025. Available online: https://www.gurobi.com (accessed on 7 February 2025).
62. Hexaly SAS. *Hexaly Optimization Solver*, Version 13.5; Hexaly: Brooklyn, NY, USA, 2024. Available online: https://www.hexaly.com (accessed on 10 October 2024).
63. LocalSolver. Hexaly: A New Generation Optimization Solver. 2023. Available online: https://www.hexaly.com/docs/last/quickstart/hexalyoptimizerintroduction.html (accessed on 15 April 2025).
64. Reingold, E.M.; Strassen, V.; Rabin, M.O.; Reingold, E.M.; Stocks, A.I.; Fiduccia, C.M.; Paterson, M.S.; Winograd, S.; Brent, R.P.; Schultz, M.H.; et al. Complexity of computer computations. *Reducibility Comb. Probl.* **1972**, *23*, 85–103.
65. Mohabbati-Kalejahi, N.; Yoon, S.W. Parallel machines scheduling problem for minimization of maximum lateness with sequence-dependent setup times. In Proceedings of the IIE Annual Conference Proceedings, Nashville, TN, USA, 30 May–2 June 2015; Institute of Industrial and Systems Engineers (IISE): Peachtree Corners, GA, USA, 2015; p. 837.

66. Land, A.H.; Doig, A.G. An automatic method for solving discrete programming problems. *Econometrica* **2010**, *28*, 497–520. [CrossRef]
67. Benoit, F.; David, T.; Van Hentenryck, J. Localsolver: A black-box local-search solver for combinatorial optimization. In Proceedings of the 25th International Conference on Principles and Practice of Constraint Programming, Stamford, CT, USA, 30 September–4 October 2019; pp. 45–60.